JMEPEG (2006) 15:255-274
DOI: 10.1361/105994906X108756

1059-9495/$19.00

Boiler Materials for Ultra-Supercritical Coal Power Plants—Steamside Oxidation

R. Viswanathan, J. Sarver, and J.M. Tanzosh

(Submitted December 9, 2005; in revised form December 20, 2005)

The corrosion behavior of tubing materials carrying steam at high temperature is of great concern to fossil power plant operators. This is due to the fact that the oxide films formed on the steam side can lead to major failures and consequently to reduced plant availability. The wall loss of the pressure boundary caused by oxidation can increase the hoop stresses and cause premature creep failures; second, the increased insulation of the tubes due to the low thermal conductivity of the oxide film can lead to increased metal temperature, thereby exacerbating the fireside corrosion as well as creep problems. The third concern is that thicker oxides may spall more easily when the plant is cooled down. On restart, the spalled material may lodge somewhere in the system with the potential for causing tube blockages, or it may be swept out with the working fluid and enter the steam turbine causing erosion damage to the turbine nozzles and blades. Failures of tubing and turbine components by these mechanisms have been widely reported in the United States. In view of the importance of the steamside oxidation, a major study of the phenomenon is being carried out as part of a major national program sponsored by the U.S. Department of Energy and the Ohio Coal Development Office. As a prelude to the experimental work, a literature survey was performed to document the state of the art. Results of the review are reported here.

Keywords boilers, corrosion rates, high temperature, oxidation, steam

1. Introduction

The efficiency of conventional boiler-steam turbine fossil power plants is a strong function of the steam temperature and pressure. Research to increase both has been pursued worldwide, since the energy crisis in the 1970s. The need to reduce CO_2 emission has recently provided an additional incentive to increase efficiency. Thus, steam temperatures of the most efficient fossil power plants are now around 600 °C (1112 °F), which represents an increase of about 60 °C (108 °F) in 30 years. It is expected that steam temperatures will rise another 50-100 °C (90-180 °F) in the next 30 years. The main enabling technology is the development of stronger high-temperature materials capable of operating under high stresses at ever-increasing temperatures. One of the major limiting factors in using materials is their susceptibility to oxidation on the steamside (Ref 1).

The corrosion behavior of materials in steam at high temperature is of concern mainly due to the thickness of the oxide films that are formed. With increasing temperature, the films form more quickly and grow to a greater thickness in a given time, leading to three potential concerns. First, the wall loss of the pressure boundary can increase the stress and cause creep ruptures. Second, the increased insulation of the tube material from the cooling fluid by the low thermal conductivity of the oxide film leads to an increase in metal temperature; thus, the potential for increased corrosion and creep rates on the flue gas side. The third concern is thicker oxides may spall more easily when the plant is cooled down. On restart, the spalled material may lodge somewhere in the system with the potential for causing tube blockages, or it may be swept out with a working fluid and eventually enter the steam turbine where erosion damage occurs to the steam path components. Loss of plant availability due to tube overheating resulting from oxide formation as well as subsequent exfoliation have been reported in austenitic and ferritic steel tubing for nearly 30 years (Ref 2, 3). In the United States (US), solid particle erosion (SPE) of turbine nozzles due to exfoliated scales has also been widely prevalent. Both problems have been on the increase in the US. Several failures of T91 alloy tubing due to long term overheating have been reported. A combination of changes in operating practices, with extended running at near to full load, longer periods between scheduled maintenance, the trend toward higher steam temperatures and pressures and plant cycling, have contributed to mounting concerns over the increasing thickness of steamside oxide scales. It is notable that long-term overheating failures due to flow restriction from exfoliated oxide scale is the second most important cause of boiler tube failures and reduced plant availability worldwide (Ref 2, 3).

Oxidation resistance of materials in steam is governed principally by alloy composition, temperature, and time. In addition, heat flux, steam pressure, steam chemistry, surface preparation of materials, grain size, surface residual stresses, impurities in the alloy, and many other variables are known to affect the oxidation to a lesser degree. A systematic compilation of these effects is lacking. Additionally, there is a need to consolidate and analyze recent data published piecemeal on a number of advanced tubing materials. This literature overview is aimed at meeting these needs. More specifically, the objectives of this overview are to identify the relative oxidation resistance of SH/RH tube alloys, temperature limits for usage in steam, and the effects of various factors on steamside oxi-

R. Viswanathan, EPRI, Palo Alto, CA 94304; and **J. Sarver** and **J.M. Tanzosh,** The Babcock & Wilcox Company Barberton, OH 44203. Contact e-mail: rviswana@epri.com.

Table 1 Candidate alloys for advanced supercritical plants

Trade designation	Nominal composition	ASME code/code case	Preferred application(a)	Temperature of application (metal)(b)
HCM2S	2-1/4Cr-1.5W-V	2199	WW	Up to 575 °C (1050 °F)
Tempaloy F-2W	2Cr-1W-Mo-V-Nb	…	WW	
HCM12	12Cr-1Mo-1W-V-Nb	…	WW	
NF12	11Cr-2.6W-2.5Co-V-Nb-N	…	H	Up to 650 °C (1200 °F)
SAVE12	12Cr-W-Co-V-Nb-N	…	H	
NF616 (P-92)	9Cr-2W-Mo-V-Nb-N	2179	H	Up to 620 °C (1150 °F)
HCM12A (P-122)	12Cr-1.5W-Mo-V-Nb-N-Cu	2180	H	
E911	9Cr-1Mo-1W-V-Nb-N	…	H	
Austenitic steels				
SAVE25	23Cr-18Ni-Nb-Cu-N	…	T	620-675 °C (1150-1250 °F)
NF709	20Cr-25Ni-Nb-Ti-N	…	T	
Hr3C	25Cr-20Ni-Nb-N	2113	T	
Super304H	18Cr-8Ni-W-Nb-N	…	T	
347HFG	18Cr-10Ni-Nb	2159	T	
800HT	21Cr-32Ni-Al-Ti	1987	T	
HR120	Ni-33Fe-25Cr-N	2315	T	
Ni Base alloys				
INCO740	24Cr-20Co-2Ti-2Nb-V-Al	…	P, T	675-788 °C (1250-1450 °F)
230	22Cr-14W-2Mo-La	2063	P, T	
Marco alloy				
625	21.5Cr-9Mo-5Fe-3.6Nb-Al-Ti	1409	P, T	
617	22Cr-12.5Co-9Mo-1.2Al	1956	P, T	
HR6W	23Cr-6W-Nb-Ti	…	P, T	
45TM	27Cr-23Fe-2.75Si	2188	P, T	

(a) WW, water wall; T, superheater/reheater tubes; P, pipes and headers. (b) These upper limit metal temperatures are based on creep. Source: Ref 4

dation. The amount of literature pertaining to the subject is enormous, and it is unrealistic to cover every publication. Key results from the literature review along with some of the results of the on-going U.S. Department of Energy study are presented.

2. Results of Literature Review

The concerns about oxidation and exfoliation can be generally addressed by careful boiler design, including materials selection, as well as boiler operation. Wherever possible, ferritic steels are preferred over austenitic steels due to their higher thermal conductivity and lower coefficient of thermal expansion (CTE). However, when the oxide scale spalls from ferritic steels, usually the complete scale thickness is involved. This process exposes fresh metal surface to the working fluid and results in a rapid initial rate of reoxidation. Repetition of this spallation-reoxidation process can result in the process of metal loss occurring at an almost linear rate, compared with the parabolic rate expected when an adherent scale is formed. For austenitic steels, the greater CTE difference between the metal and the oxide provides the potential for increased cracking and spalling of the scale, in general, only the outer layer of the scale is spalled, leaving the inner rate-controlling layer intact so that the effect of a single scale spalling event is less on these alloys.

Currently, low-chromium (2-3% Cr) alloys are limited in boiler service to temperatures of 565 °C (1050 °F) to 600 °C (1115 °F) due to oxidation loss from the fireside (Ref 4). Ferritic alloys in the 9-12% class, such as T91, T92, and HCM 12, appear to be capable of use up to 620 °C (1150 °F). More advanced ferritic steels, such as T 122 (HCM 12A) and VM12, may be suitable up to temperatures above 620 °C (1150 °F) (Ref 5). The temperature limits imposed by the US boilermakers on the 300-series stainless steels (10-17%Cr) range from 700 °C (1292 °F) up to the ASME Boiler and Pressure Vessel Code creep rupture-based limit of 816 °C (1500 °F) (Ref 6), although for conventional superheater tubing, the limit of operation is usually to a maximum of 675 °C (1250 °F). At the higher temperatures, the advanced stainless steel grades will find use. However, fireside corrosion will likely prove to be the temperature limiting factor in US boiler designs.

The key ferritic steels, austenitic stainless steels, and nickel-based alloys of interest for advanced coal power plants are presented in Table 1 (Ref 4). A more complete listing of alloy composition of alloys may be found in Ref 4. Some of these alloys are currently being used in fossil boilers operating at temperatures over 600 °C (1112 °F), and some are being considered for potential use in ultra-supercritical power plants operating at steam temperatures above 700 °C and pressures above 25 MPa. The oxidation behavior of these steels is reviewed in the following sections.

3. Ferritic Steels

3.1 Kinetics of Oxidation

There is general consensus that steamside oxidation of ferritic boiler tubes occurs at a rate that can be represented by the following model:

$$\text{Scale thickness } x = Kt^n \quad \text{(Eq 1)}$$

where x is the oxide scale thickness; t is the exposure time; K is the proportionality coefficient, which is a function of temperature, alloy composition, oxygen partial pressure, stress level, and radius of curvature of the tubing; and n is the rate

Table 2 General forms of the oxide correlation for low alloy Cr-Mo steels

General form of expression(s)	Approximate oxide-growth law
Rehn and Apblett (Ref 9): Log x = A + B (LMP)	$x = k(t)^{1/3}$
Paterson and Rettig (Ref 10): Log x = A + B (LMP)	$x = k(t)^{1/2.1 \text{ to } 1/2.6}$
Dewitte and Stubbe (Ref 11): $x^2 = kt$	$x = k(t)^{1/2}$
Paterson (Ref 8): $x = k(T, A, P)^{1/2.6 \text{ to } 1/3.0}$	$x = kt^{1/2.6 \text{ to } 1/3.0)}$

x, oxide scale thickness; t, time; k, oxide scale growth law rate constant; A, B, C, and D, coefficients; LMP, Larson-Miller parameter; T, temperature; P, bulk steam pressure. Note: Oxide scale thickness = 2.4 metal loss (penetration). Source: Ref 7, 12

exponent. For ferritic tubing, n has been found to vary from 1/2 to 1/3, as shown in Table 2 and is believed to be a function of time and temperature (Ref 7-12). All the correlations, except those of DeWitte and Stubbe, were developed based on data obtained on tubes returned from boiler service. The DeWitte and Stubbe correlations were derived from data in air in laboratory tests.

In low alloy ferritic steels (typically 0-2% Cr), a double-layer scale consisting of magnetite (Fe_3O_4) and hematite (Fe_2O_3) is formed depending on the alloy composition and partial pressure of oxygen when the metal temperature is below approximately 580 °C (1076 °F). At higher temperatures, an additional inner layer of wustite (FeO) may be present (Fig. 1). With increasing temperature, wustite (FeO) formation increases. The wustite transformation temperature is variously cited as 570 °C (1050 °F) for carbon steel, 585 °C (1085 °F) for 1-1/4Cr1/2Mo steel (Ref 11), and 595 °C (1103 °F) (Ref 11), or 615 °C (1140 °F) (Ref 12), for 2-1/4Cr1Mo steel by different reports.

Because different investigators report results in terms of different criteria such as oxide scale thickness, metal loss, or penetration, the following empirical correlations are often used for low alloy steels with bilayer oxides (Ref 12):

- Inner layer thickness = metal loss
- Outer magnetite layer thickness = 1.4 times the thickness of the inner layer
- Total scale thickness = 2.4 metal loss

At temperatures close to 580 °C, it has been suggested that in 2-1/4Cr1Mo steel boiler tubes, the transition to linear kinetics may occur in 8,000-16,000 h (Ref 8, 10). Most of the oxidation studies in steam tend to suggest that parabolic kinetics prevail at temperatures up to 700 °C (1292 °F). At higher temperatures, however, linear kinetics are believed to take over. One study (Ref 13) using model alloys in water vapor-Ar mixtures has reported linear kinetics for Fe-Cr alloys containing up to 15% Cr over temperatures in the range 700-1200 °C (1292-2192 °F). Likewise, earlier studies (Ref 13, 14) of model Fe-Cr alloys suggested that linear kinetics prevailed at temperatures above 700 °C (1292 °F) for Cr levels in the range 1-15%. Effertz and Meisel (Ref 15) and Manning and Metcalfe (Ref 16) concluded that the growth in oxide thickness with time

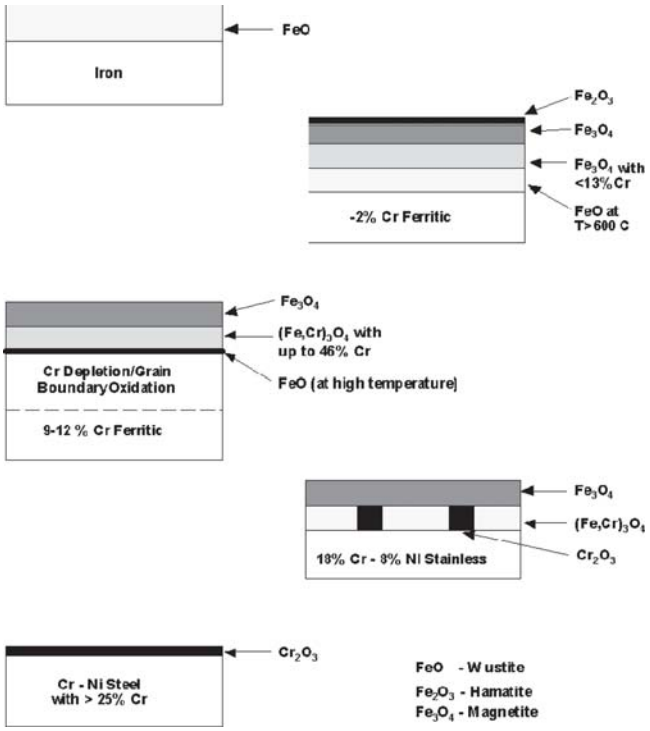

Fig. 1 General summary of the oxide morphology formed in high temperature steam

was adequately described by a parabolic oxidation law. Eberle and Kitterman examined the scaling behavior of 2-11% Cr alloys at 593 and 649 °C (1100 and 1200 °F) (Ref 17). Their data indicated that parabolic oxidation kinetics prevailed for only about six months, following which the rate became constant. Grobner et al. (Ref 18) also noted a transition from parabolic to linear kinetics in steam oxidation studies.

From the above discussion, it is clear that the data in the literature on corrosion rates of low alloy ferritic steels (0-2-1/4% Cr) do not present a clear picture of the effect of exposure time. Initially, parabolic kinetics seem to prevail, but the time and temperature at which transition to linear kinetics occurs has not been clearly established because it can be a function of the alloy content, environment, heat flux, and other variables. It appears that the transition could occur at temperatures as low as 500 °C after 8,000-16,000 h. Whether the transition is strictly caused by wustite formation or whether periodic spalling could also be an additional factor in boiler tubes is unclear.

Data based on service returned tube samples suggest cubic, linear, and other forms of oxide growth, whereas laboratory tests conducted isothermally suggest parabolic oxide growth at temperatures up to 700 °C. It is likely that the transition from parabolic behavior starts with the onset of wustite formation, but is not complete until wustite becomes the dominant oxide in the scale. This would suggest a range of behavior over a range of temperatures, 580-700 °C in the case of 2-1/4Cr-1Mo steel. It is also possible that exfoliation of scales occurs more readily in service and changes the kinetics of oxidation with time. Unlike laboratory isothermal oxidation, rates obtained from field tests provide the most realistic data.

For 9-12% Cr steels NF12, NF616, and HCM12A in the range 600 °C (1112 °F) to 750 °C (1382 °F), Muramatsu et al. have observed parabolic kinetics (Ref 19); and Kajigaya et al. have reported parabolic kinetics in steam for 9-12% Cr steels at

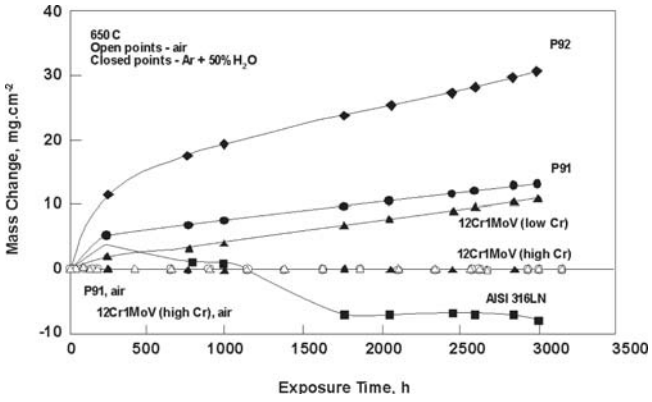

Fig. 2 Mass change data for Cr steels exposed in Ar-50% H_2O and in air at 650 °C showing the superior oxidation resistance of 12% Cr steels compared to 9% Cr steels at 650 °C (1200 °F) (Ref 22)

600 °C (1112 °F) and 650 °C (1200 °F) (Ref 20). Naoi et al. (Ref 21) have reported parabolic kinetics for NF616, T91, and HCM12 based on tests in the range 500 °C (932 °F) to 799 °C (1300 °F) for 3000 h in steam. Parabolic kinetics for advanced 9-12% Cr steels have also been reported by Quadakkers et al. (Ref 22) at 650 °C in Ar + 50% H_2O (Fig. 2). It is claimed that this environment simulates the oxidation behavior in steam and is much more aggressive than dry air.

Khanna et al. (Ref 23) observed that the oxidation rate for 9% Cr steels followed parabolic kinetics at all temperatures studied from 500-800 °C (932-1472 °F). The rate of oxidation was found to be lower at 800 °C (1472 °F) than at 700 °C (1292 °F). This inversion phenomenon has been reported by other researchers (Ref 24, 25) and was attributed to the higher Si content (0.41-0.90 wt.%) in these alloys. Tamura and Fukuda (Ref 26, 27) have also reported parabolic oxidation kinetics for 8-12% Cr steels. Evidence in the literature clearly suggests that for 9-12% Cr steels, only parabolic kinetics prevail at temperatures at least up to 700 °C (1300 °F), and perhaps even up to 800 °C (1475 °F), in laboratory studies.

The maximum mass gain of ferritic materials containing 1.1-8.7% Cr when tested at 538 °C (1000 °F) for 10,000 h was 10 mg/cm (Ref 28). These alloys formed tenacious and nonspalling oxides when tested in supercritical steam. Similarly, a variety of Cr-Mo steels containing 2-11% Cr were exposed to superheated steam at 482-538 °C (900-1000 °F) for 28,000 h (Ref 29). The alloys oxidized at decreasing rates for about the first year, after which the rates became low and constant. The oxidation rate did not exceed 11 μm/year (0.5 mpy).

The oxidation kinetics for ferritic steels can be illustrated by the plot shown in Fig. 3. In this plot, the line that divides linear kinetics from parabolic kinetics is not distinct because factors other than temperature and Cr content (e.g., other alloying elements, other environmental factors, heat flux, etc.) play an important role in determining oxidation kinetics.

Wright and Pint (Ref 6) made comparisons of the relative amounts of oxide growth expected, assuming parabolic or linear oxidation behavior. The mass gains and corresponding oxide thicknesses (assuming no scale spallation) expected in the nominal plant lifetime of 250,000 h are summarized in Table 3 [assuming an average metal temperature of 650 °C (1202 °F) and no effect of steam pressure]. Spallation would result in regrowth of oxide at a faster rate that, in the case of parabolic kinetics, would depend on the thickness of the remaining oxide.

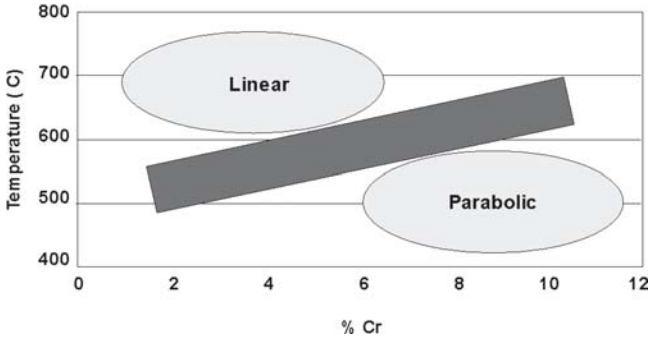

Fig. 3 General trend of oxidation kinetics for ferritic steels as a function of %Cr and temperature

An assumption of linear oxidation kinetics results in significantly greater oxidation (and much shorter component life) than would be realized from an assumption of parabolic kinetics.

3.2 Activation Energy for Oxidation

Parabolic rate constants were calculated by Wright and Pint (Ref 6) from plotting the literature data on mass gain-square root of time coordinates for alloys with Cr contents in the ranges of 0-2% Cr and 9-12% Cr. The assumption was made that the oxidation kinetics could be described by the usual relationship:

$$\text{Scale thickness} = A \cdot e^{-Q/RT} \cdot t^n \quad \text{(Eq 2)}$$

where Q is the activation energy for the rate-controlling process, T is the metal temperature (absolute); t is time; A is the Arrhenius constant; and R is the gas constant.

In 0-2% Cr alloys, the trend of these data was represented by two straight lines that intersected at approximately 500 °C (932 °F), with a significant increase in oxidation rate in the higher temperature regimen. The calculated activation energy for the oxidation process below 500 °C (932 °F) was 85 kJ/mol, and above 500 °C (932 °F) it was 235 kJ/mol. In 9-12% Cr alloys, a single rate-controlling oxidation process operated over the whole temperature range studied [290-700 °C (554-1292 °F)], with an activation energy of 146 kJ/mol. This is entirely in contrast to the results of Watanabe et al. (Ref 30).

Watanabe et al. (Ref 30) investigated oxidation behavior of STBA24, HCM2S (T23), NF616 (T92), and HCM12A (T122) in steam in an autoclave in the range 560-700 °C. The low alloy steels STBA24 and HCM2S (T23) showed the same activation energy, i.e., 350-400 kJ/mol, over the entire temperature range. On the other hand, the 9% Cr and 12% Cr alloys showed a bilinear behavior. Below 600 °C they had the same Q but exhibited much lower Q values in the range 600-700 °C; the higher the Cr, the lower the Q. HCM12A had a value of 40 kJ/mol (Fig. 4).

In 9-12% Cr alloys, an activation energy of 199 kJ/mol was observed (Ref 6), whereas a lower value of 103 kJ/mol was observed in studies that used Ar-0.1 water. Wright and Pint reported that the activation energies determined from the assumption of parabolic kinetics for both 0-2% Cr and 9-12% Cr alloys do not provide any clear-cut indication of the rate-controlling mechanism because they fall into the top of the range reported for Fe diffusion in FeO and into the bottom of

Table 3 Summary of oxidation rates

Alloy	Temperature range, °C	Parabolic oxidation(a)(c) A	Parabolic oxidation(a)(c) Q, kJ/mol	After 205 kh at 650 °C(b) Mass gain, mg/cm^2	After 205 kh at 650 °C(b) Oxide thickness (d), μm
0 to 2% Cr	500-700	2.10×10^{4}	235	977	520
9 to 12% Cr	450-700	1.42×10^{-2}	146	263	140
NF616	500-700	2.35×10^{-10}	162	ND	ND
9 to 12% Cr	470-1200	3.70	157	4,332	2,307
	700-1200(b)	5.5×10^{-2}	113	19,914	10,605
9 to 12% Cr	450-1200	230.5	199	1,133	603
	700-1200(b)	1.28×10^{-2}	103	17,059	9,085

(a) From $k = A \cdot e^{-Q/RT}$. (b) Assuming oxide is all magnetic ($p = 5.18$ g/cm^3). (c) A in g^2/cm^{4}s. (d) A in g/cm^{2}s. Source: Ref 6

the range for Fe diffusion in Fe_3O_4 (Ref 3). When linear kinetics is assumed, the results for the 0-2% Cr alloys straddle the values for Fe diffusion in FeO. The activation energy from the overall fit for the 9-12% Cr alloys was typical of those reported for Fe diffusion in Fe_3O_4, whereas the activation energies from consideration of only the Ar-0.1 water vapor data were lower than this.

3.3 Effect of Composition

There is ample evidence in the literature to suggest that with Cr concentrations between 2 and 9%, at temperatures below 600 °C (1112 °F) corrosion behavior in superheated steam is independent of Cr content (Ref 29). The difference between 9% Cr steels and 12% Cr steels is also nominal at 600 °C (1112 °F) but becomes marked at 650 °C (1200 °F). Eberle and Kitterman (Ref 17) have reported that at 593 °C (1100 °F), the differences in scaling resistance between 2 and 9% ferritic steels is too small to be significant for most steam applications. At 650 °C (1200 °F), on the other hand, differences in the scaling rates of the ferritic steels became marked. The scaling rate of the 9Cr-1Mo steel at 650 °C (1200 °F) was only 1.5 times that at 593 °C (1100 °F), whereas the scaling rates of the other steels increased at 650 °C (1200 °F) by three- to fourfold. These trends are illustrated in Fig. 5. Solberg et al. (Ref 31) measured the loss of metal in steam at 595 and 650 °C (1103 and 1202 °F). Their results showed that at 595 °C (1103 °F), there was no significant effect on metal loss between 1 and 9% Cr steels, but significant improvement in oxidation resistance was observed between 9 and 12% Cr steels. These effects were less pronounced at 650 °C (1202 °F).

In Fig. 6, the behavior of ferritic steels is contrasted with austenitic steels (Ref 19). Unlike the 9-12% Cr ferritics, the austenitic steels are characterized by a single activation energy over the entire temperature range, with the caveat that as Cr concentration increases, Q decreases.

Paterson, Moser, and Rettig (Ref 8) evaluated the relative performance of several CrMo steels in the laboratory based on failed boiler tubes (Fig. 7). Based on these results, they derived the values of the scaling factors using 2-1/4Cr-1Mo steel as having an index of one. On this basis, the scaling factor for 9% Cr is 2.5. This effect of Cr is rather small, consistent with other results.

In a recent study by Watanabe et al. (Ref 30) oxidation kinetics of recently developed ferritic steels that contain either 2.2%, 9%, or 11% Cr and about 2% W HCM2S, NF616, and HCM12A, respectively, were investigated in the temperature range of 560-700 °C and steam pressure in the range of 1-10 MPa in pressurized superheated steam to determine the effects of chemical composition of the steels. Contribution of Cr to oxidation resistance was pronounced above 600 °C, while no material dependency of the oxidation rate was found at 600 °C or lower. The apparent activation energy for the oxidation rate clearly changed at around 600 °C for NF616 and HCM12A. In contrast, HCM2S displayed a single activation energy over the entire range of temperatures. Although temperature and chemical composition of the steels were the major factors, steam pressure also showed an adverse effect on the oxidation rate in the lower temperature range, 570-600 °C. The behavior of STBA24 and HCM2S were identical, indicating that W has no significant effect. Nakagawa et al. (Ref 20) confirmed the finding that scale growth in 9-12% Cr steel is parabolic and that the differences between 9% and 12% Cr steels is more clearly delineated only above 600 °C (Fig. 8).

The effect of Cr and Si contents on the steam oxidation behavior of high Cr ferritic steels was also reported by Tamura and Fukuda et al. (Ref 26, 27). They reported parabolic oxidation kinetics for all the tested 8-12% Cr alloys. Silicon was found to be more effective than Cr in decreasing the parabolic rate constant of high Cr ferritic steels above 650 °C (1202 °F). A continuous Cr-rich layer accompanying Si segregation was consistently observed in the inner oxide scale at the metal/oxide interface with the materials of higher steam oxidation resistance. An appropriate addition of Si to high Cr ferritic steels seems to promote the formation of the Cr-rich inner scale layer and its stability in a double layered scale, the outer scale was Fe-rich and the inner scale Cr-rich. Quadakkers et al. (Ref 22) also reported that the oxidation resistance of 9-11% Cr can be improved by increasing the amount of Cr, Si, and/or Al. However, protective surface scale formation on this basis requires additions of 1-2% Al or Si. Such high additions of these elements can lead to embrittlement of the steels. Just as Si is one of the most effective elements to improve the steam oxidation resistance of ferritic steels (Ref 27), it can deteriorate a steel's creep strength at elevated temperatures. Therefore, Si additions must be maintained within a specific range to keep a good balance between oxidation resistance and creep strength. Test results suggest that a proper Si content is 0.3%, as Si contents above 0.4% would be detrimental to toughness (Ref 27). The effect of Si on the oxidation resistance of 0.25C-1Cr-0.25Mo0.15V steel in steam was investigated by Kharina et al. (Ref 32). They indicated that Si in the range of 0-3% has an irregular influence on the oxidation rate at 500-600 °C (932-1112 °F). The usual amount of about 0.3% Si, however, proved

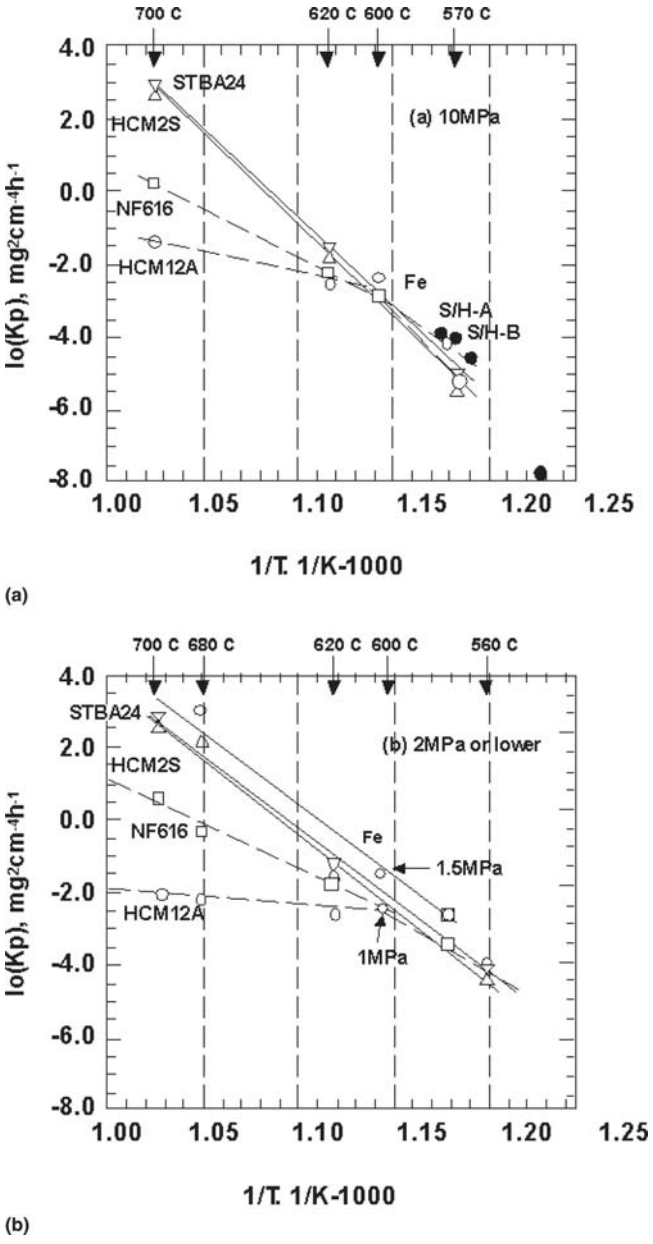

Fig. 4 Arrehnius-type plots of K_p measured at (a) 10 MPa and (b) 2 MPa or lower (2%). The figure shows relatively marginal effects of steam pressure. Cr level effects become marked only above 600 °C (1112 °F) (Ref 32).

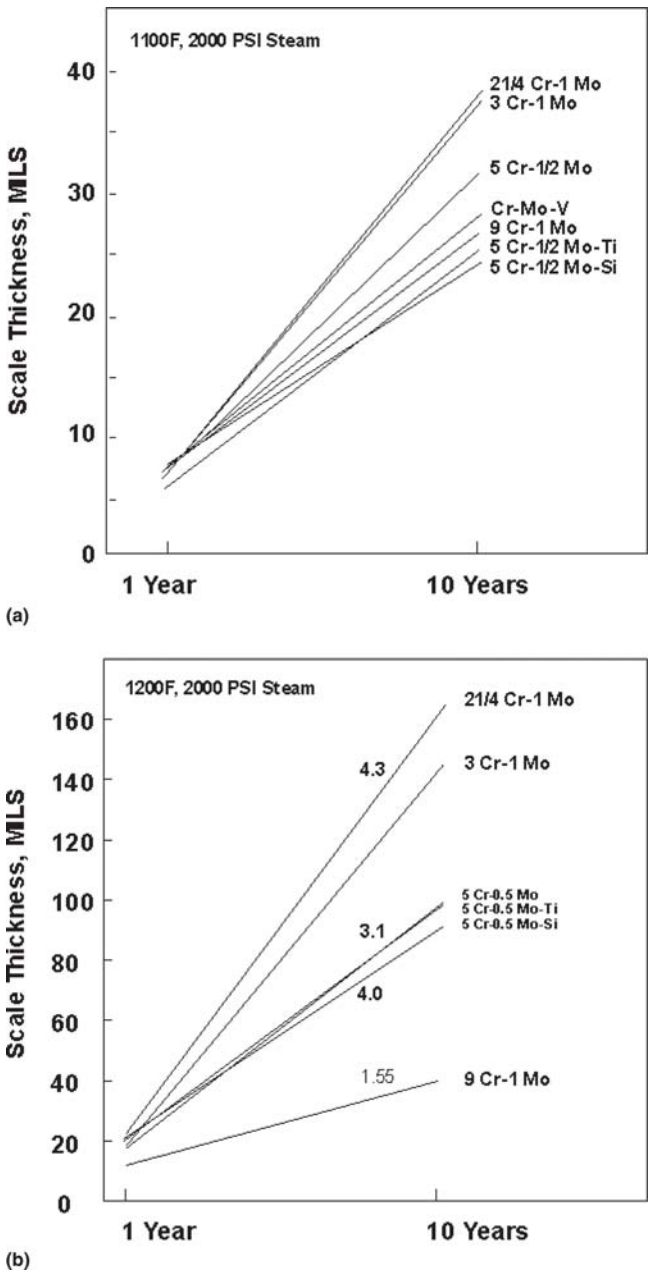

Fig. 5 Calculated scale thicknesses for 10 year exposure of ferritic steels in steam at (a) 593 °C (1100 °F) and (b) 650 °C (1200 °F); the numbers are the 650 °C/593 °C scale thickness ratios. Cr effects become pronounced only at 650 °C (1200 °F) (Ref 17)

beneficial above 500 °C (932 °F). Preoxidation of the Si-modified alloy in an Ar-O_2 mixture also greatly improved its oxidation resistance in steam at 700 °C (1292 °F) in 1000 h tests. The beneficial effects due to Si have also been verified recently by Sato et al. (Fig. 9; Ref 33).

The combined beneficial effects of Cr and Si have recently been investigated by Naoi et al. (Ref 21). Steam oxidation tests of NF616, T91 and 12% Cr steel were carried out at temperatures of 500-700 °C (932-1300 °F) for up to 3000 h. As is usually observed in ferritic steels, the oxide on NF616 consisted of two layers, the outer layer of Fe_3O_4 and inner of $(Fe,Cr)_3O_4$. The growth rate of steam oxide scale was evaluated based on the parabolic law as a function of temperature and Si and Cr content. The coefficients of the formula were determined by regression analysis. Predictions from these equations, however, did not agree with the results from field tests lasting up to 44,000 h.

Murata and others found that the presence of S and an impurity content level leads to a tremendous improvement of the steam oxidation resistance of high Cr ferritic steels at 650 °C (1202 °F) (Ref 34, 35). After testing in steam at 650 °C for 1000 h, an 11% Cr steel containing 0.009% S exhibited approximately half of the oxide thickness of an 11% Cr steel containing 0.001% S. The oxide thickness decreased sharply with increasing S until the S content reaches 0.005% (50 ppm) and then decreased gradually with increasing S content (Fig. 10). Sulfur was found to be a more effective element in improving oxidation resistance than Si. Therefore, the S content

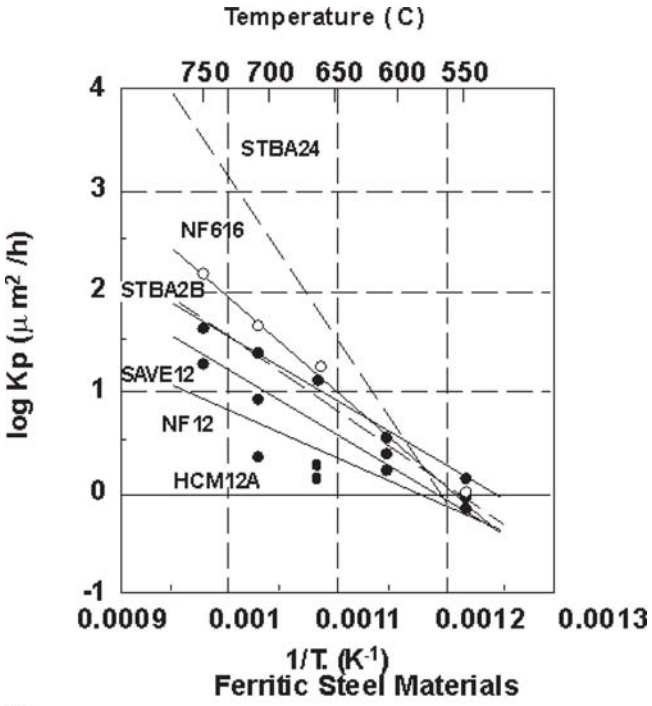

(a)

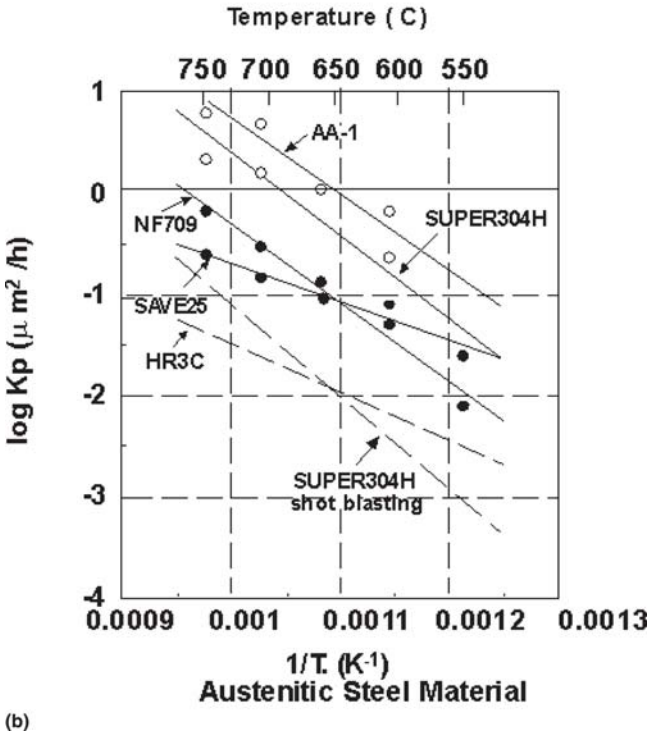

(b)

Fig. 6 Steam oxidation scale growth rate K_p of candidate materials versus temperature (Ref 19); unlike the 9-12% Cr ferritics, the austenitic steels exhibited a single value over a large temperature range.

should be controlled to remain in the range of 0.005 to 0.01% in high Cr ferritic steels to improve the oxidation resistance without producing any harmful effect on the mechanical properties. The beneficial effect due to S was realized only when it was present as chromium sulfide and not in solid solution. The mechanism by which S improves oxidation resistance remains unclear (Ref 36).

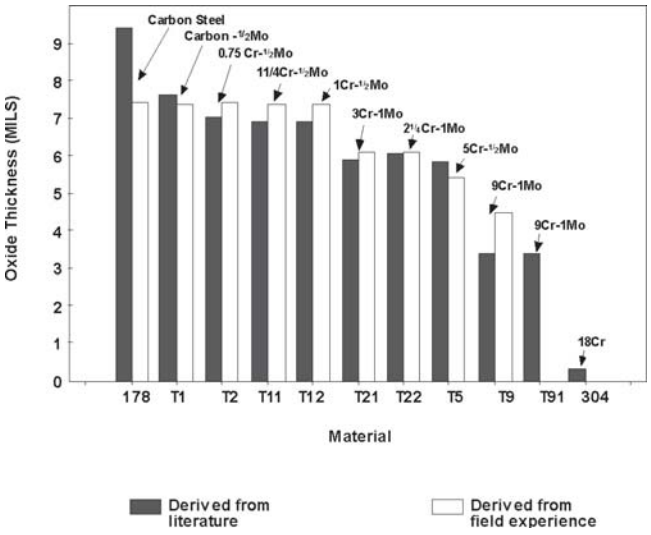

Fig. 7 Estimated oxide thickness of different tube alloys made using literature derived and field experience derived alloy coefficients (Ref 8); the figure shows relative scaling factors using 2-1/4Cr-1Mo as the benchmark.

Osgerby and Fry (Ref 37) found beneficial effects from Si and Mn. They proposed a chromium equivalent containing Cr, Si, Mn, and Mo as beneficial elements, and W as a detrimental element. The mass loss results in 600 and 650 °C tests on several 9-11% Cr steels correlated well with the W content.

Manganese was also found to significantly contribute to the formation of protective oxide scales in 9-12% Cr steels in water vapor containing gases in the temperature range of 550-800 °C (1022-1472 °F) (Ref 38). Higher temperatures result in enhanced diffusion of the Cr and Mn in the scale, generally resulting in the formation of more protective oxides, at least up to an exposure time of 100 h. The oxidation resistance of 9% Cr steels during oxidation in steam at 650 °C (1202 °F) was also improved with the addition of Pd (Ref 39, 40). Palladium was found to promote the formation of Cr-rich oxide scale. Itagaki et al. (Ref 41) reported significantly improved oxidation resistance in steam at 650 °C (1202 °F) in a 9% Cr-based alloy (NF616) to which an addition of 3% Pd had been made. Itagaki et al. reported a 1.3 × increase in mass gain when W was substituted for Mo in 9% Cr-based alloys, whereas Watanabe et al. (Ref 30) reported that an addition of 1.6% W to a 2% Cr steel made no difference to the oxidation rates in their tests (Ref 41). To maximize the creep rupture strength of a 9% Cr steel without degrading its toughness, the W concentration should not exceed about 3% (Ref 40).

The effect of water vapor content on the 650 °C (1202 °F) oxidation behavior of 9% Cr steels alloyed with varying concentrations of Si, W, and Mo has been investigated (Ref 42). Mass gain in the test materials generally increased with increasing water vapor content. Increased Si concentrations decreased the mass gain in water vapor. Additions of W and Mo also appeared to have a beneficial effect. This is contrary to the findings of Watanabe et al. where W effects were insignificant, and that of Osgerby et al., where W led to adverse behavior in ferritics (Ref 37). These authors, however, reported beneficial effects due to W in Ni-base superalloys.

The effect of B on the oxidation of Fe-9Cr-1Mo alloys in high temperature steam was noted by Rowley at al. (Ref 43). Boron confers protection to low-Cr steels in high temperature

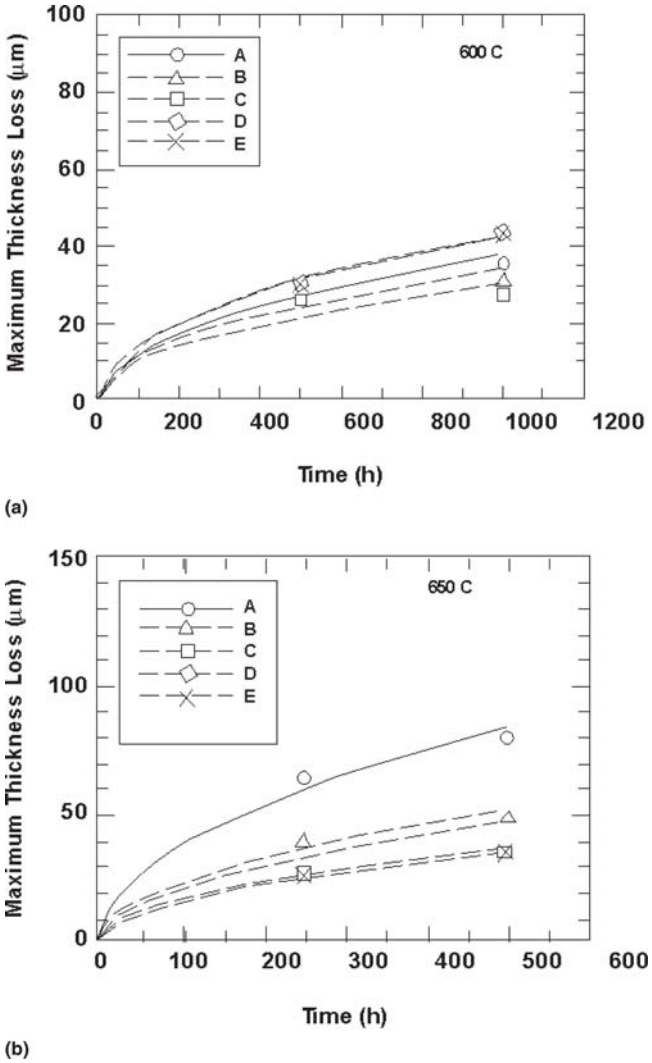

Fig. 8 Maximum thickness losses of 9-12% Cr steels exposed to (a) 600 °C and (b) 650 °C steam. Steels A and B contain about 8.5% Cr while C, D and E contain 11.5% Cr. The effect of Cr level is minimal at 600 °C but becomes marked at 650 °C (Ref 20).

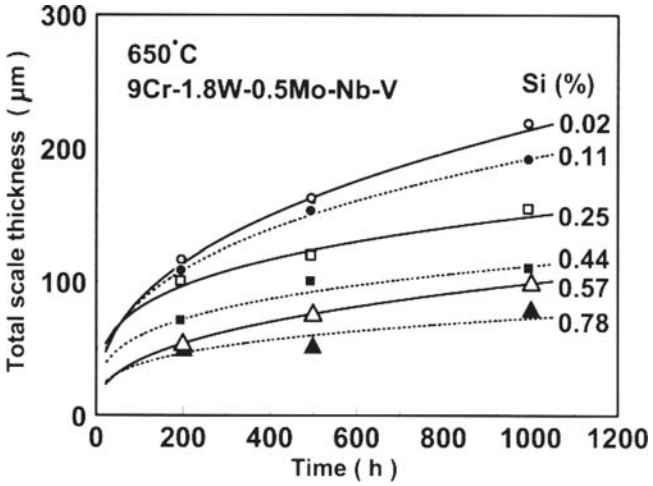

Fig. 9 Effect of Si content on steam oxidation property (Ref 33)

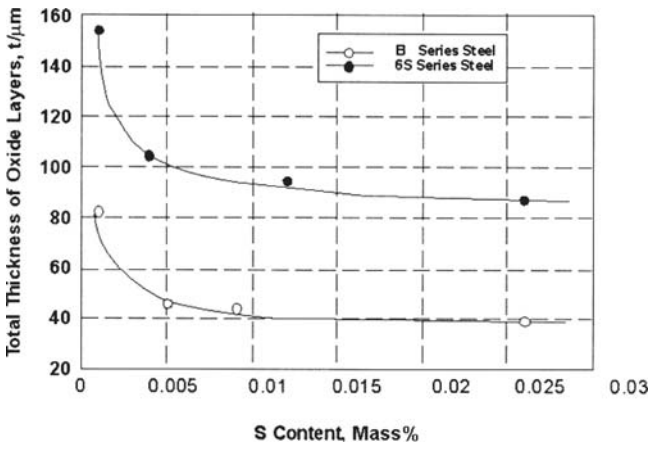

Fig. 10 Changes in the total thickness of the oxide layers with S content in the B series and the 6S series steels (11% Cr) exposed to steam atmosphere at 650 °C for 1000 h (Ref 34, 35)

[600 °C (1112 °F)] steam due to the formation of a passive microcrystalline film of composition Cr_2O_3, which resists further oxidation.

3.4 Effect of Test Variables

The test procedures used have varied widely and could have caused major differences in the results obtained by different investigators. Test variables have included heat flux, environment, steam pressure, alloy composition, and laboratory versus in-boiler field tests. These effects are briefly reviewed in this section.

3.4.1 Effect of Heat Flux. In the case of furnace tubes, the growth of a steamside scale increases the thermal barrier to the steam, and the average temperature of the steamside oxide increases in proportion to steamside scale thickness. Oxide growth therefore is accelerated because it occurs under progressively increasing temperature and not isothermally as in laboratory tests. This is particularly a concern where thick oxide scales form, such as in the case of low alloy ferritic steels. An example of this behavior is shown in Fig. 11 from the work of Griess et al. (Ref 44). The figure clearly illustrates the accelerating oxidation rates resulting from heat flux in 2-1/4Cr-1Mo steels. According to Paterson et al. (Ref 8) the so called breakaway oxidation, which in the past has been attributed to oxide cracking, may really be caused by temperature increases on the steamside of the tubes. Because a reheater tube in a boiler is larger in diameter and operates under a lower heat flux compared with superheater tubes, the temperature of the former will be less affected by oxidation. Paterson et al. (Ref 8) have modeled these differences to account for differences in remaining life under apparently similar operating conditions. It is quite clear that laboratory tests under isothermal conditions do not reproduce scale growth behavior in actual boilers. Consistent with this, steamside oxides in furnace tubes returned from service contain much more porosity than oxides formed in laboratory tests under isothermal conditions. The former scales also exfoliate more readily. This is attributed to the heat flux effect.

Very few investigators have performed both laboratory isothermal tests in steam and boiler tests under heat flux conditions for comparison studies. One such study is that of Naoi et

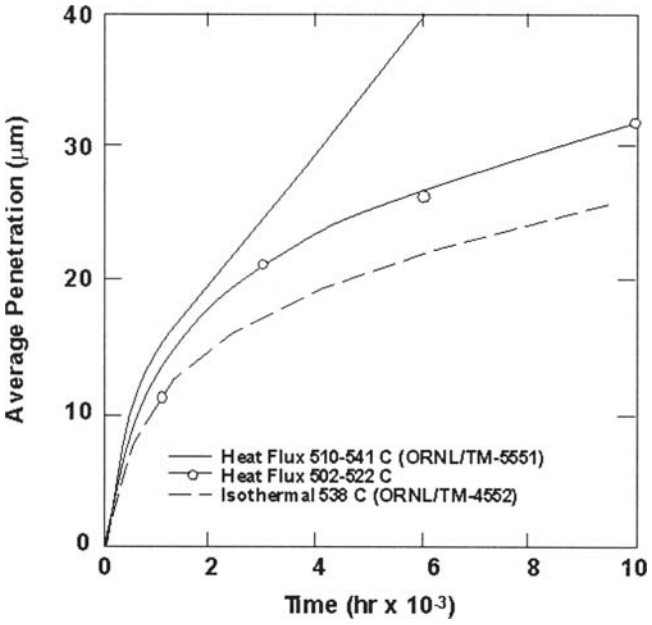

Fig. 11 Comparison of the average penetrations (metal loss) of 2-1/4Cr-1Mo steel in superheated steam under isothermal and heat transfer conditions; in both heat transfer tests, the heat flux was 126 kW/m^2 (Ref 44)

al. (Ref 21). They conducted isothermal steam oxidation tests at 500-700 °C on NF616 samples and derived rate equations. The prediction from these equations was compared with mass loss results obtained on NF616 tubing that had been installed in a tertiary superheater of a 375 MW boiler and exposed to times up to 44,456 h. The steam temperature was 569 °C (1060 °F). The steam-side oxide thicknesses after 13,763 h, 21,272 h, and 44,456 h of exposure were 255, 280, and 340 μm, respectively. The field data were found to deviate from the parabolic behavior predicted from laboratory tests.

3.4.2 Effect of Environment. Exposure procedures in common use in the laboratory in ascending order of complexity include the following (Ref 45, 46):

- Water vapor in a carrier gas (usually Ar)
- Flowing steam at atmospheric pressure
- Static steam at high pressure
- Flowing steam at high pressure

None of these laboratory procedures include heat flux for which exposure in plant is needed. Plant exposure is normally the final stage in material selection (Ref 37, 45, 46). A recent review has highlighted the scatter in data arising from the use of different exposure procedures (Ref 45). The authors of the review concluded there is no systematic variation of scale growth with laboratory exposure procedures.

In studies by Osgerby and Fry, specimens of ferritic and martensitic steels (2-1/4Cr1Mo and 9Cr1Mo-P92) were exposed to steam environments at 550, 600, and 650 °C using the different laboratory procedures. Although the scale thickness measured after a given time were similar for all the procedures, significant differences in the morphology of the oxide scales grown under different conditions could be observed. Scales grown under Ar-50% H_2O showed a compact inner spinel layer with an outer porous magnetite layer. There were traces of very thin and discontinous hematite at the surface. The scale grown under flowing steam at atmospheric pressure had a compact outer layer of magnetite with an inner spinel layer that contained a plane of massive defects. In contrast, the scale grown under high pressure static steam was compact throughout, with some evidence of roughening at the surface of the outer scale.

Diversity in the scales grown under different conditions has also been observed in the 9Cr1Mo steels. Two additional features in the scales grown on these materials are the presence of internal oxidation below the spinel under all conditions and the development of wavy scale-substrate interface and surface in the scales grown under flowing steam and static high pressure steam (Ref 46). Surprisingly, it was the structure of the scales formed under the Ar-50% H_2O mixture that was most similar to that formed in service. This procedure is the most dissimilar to the actual service conditions, so it would be expected to produce the least representative scales.

Dottenwanger et al. (Ref 42) compared oxidation rates of 9% Cr steels in dry air and in air containing 4-10% water vapor at 650 °C. Their results clearly showed that water vapor significantly accelerates oxidation. Similarly, Ennis and Czyrska-Filemonowicz (Ref 47) showed that the oxidation resistance in air was excellent due to the formation of tightly adherent, protective oxide scales. The protective scales formed in air on 9% Cr steels were identified as consisting of $(Fe,Cr)_2O_3$ and $(Fe,Cr,Mn)_3O_4$. However, in steam-containing atmospheres, the scales formed at 600 and 650 °C were thick and consisted of an external Fe_3O_4 scale and an internal two-phase scale of Fe_3O_4 and $(Fe,Cr,Mn)_3O_4$. Below the oxide scale, internal oxidation of Cr to form $(Fe,Cr,Mn)_3O_4$ occurred at the martensite lath boundaries.

Several investigators have tried to compare results of oxidation under steam and simulated combustion gas environments. Nakagawa et al. (Ref 20) conducted 100 h corrosion tests in simulated combustion gases containing 4% O_2 + 15% CO_2 + 10% H_2O with the balance N_2 using T92 and T122 steels. The SO_2 content was varied from 0, 0.01, 0.05, 0.1, and 0.25%. Tests were conducted at 600, 650, and 700 °C. Parallel tests were conducted in steam at the same temperatures. Based on mass loss results, they concluded that oxidation rates were the same in both environments as the steam content of the gas mixture was the rate controlling specie. Ennis et al. (Ref 48) reached a similar conclusion by comparing oxidation rates of T91, T92, and T122 alloys in steam and in a gas mixture similar to the above (also containing 0.01% HCl) tested at 600 and 650 °C for 10,000 h. These authors concluded that the steam content of the simulated flue gas dominated oxidation, thus producing results similar to that obtained in pure steam. Ennis et al. (Ref 48) also noted that the oxidation rate constant for ferritic steels dropped precipitously (Fig. 12) in going from 9% Cr to 12% Cr, indicating that a critical Cr level of at least 11% is needed for oxidation resistance.

Extensive laboratory and field testing of 9-12% Cr ferritic steels has been carried out to determine their corrosion behavior in air, flue gas, and steam at temperatures up to 680 °C (1256 °F) (Ref 49). The alloys tested were X20, T91, E911, and NF616. Tube sections of E911 and NF616 were incorporated into the final superheater stage of a coal-fired power station at Wilhelmshaven, Germany, and subjected to steam and metal temperatures up to 605 and 630 °C (1121 and 1166 °F), respectively, with the high-metal temperatures being

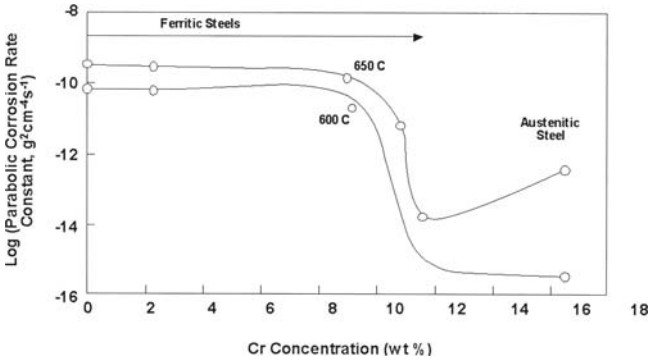

Fig. 12 The effect of Cr content on the oxidation rate of steels at 600 and 650 °C in simulated combustion gas (N_2-1%O_2-14%CO-0.1%SO_2-0.01%HCl-7%H_2O). Note: precipitous drop of K between 9 and 12% Cr steels (Ref 48)

achieved through the use of control valves. The scale thicknesses were measured at intervals. On the steam side, with a mean steam temperature of 600-605 °C (1112-1221 °F), after 11,000 h these thicknesses were 330, 460, and 325 μm (13, 18, and 13 mil) for T91, E911, and NF616, respectively. On the flue gas side, the scale thicknesses were 210, 165, and 205 μm (8, 6 and 8 mils). These differences were considered to be insignificant and within the scatter of an industrial field test. Subsequent metallographic examination indicated that, while the scale formed on X20 was uniform, dense, and protective, the scale on NF616 contained significant porosity. No outer scale was found on E911.

Air exposure tests conducted by Fleming et al. (Ref 49) up to 4000 h at 630 and 680 °C (1166 and 1256 °F) indicated that X20 (12% Cr) exhibited greater oxidation resistance than the 9% Cr group. In autoclave tests in steam at 0.7 MPa (103 psi) and 500 °C (932 °F) for times up to 3936 h, there was again little difference between the 9% Cr variants, whereas scale thicknesses were about twice those found on X20. Using the steam and flue gas data, a maximum total metal loss of 0.6 mm (24 mil) may be expected after 100,000 h. These results indicate that far more oxidation damage was experienced in the field trials than suggested by the laboratory tests. From these results, the authors concluded that none of the 9% Cr steels is suitable for long-term use as boiler tubes above approximately 600 °C (1112 °F), based primarily on the decrease in heat transfer caused by the steam-side scale rather than from the metal loss. This increase in tube wall temperature means that the strength advantages of the developmental 9% Cr steels (E911 and NF616) cannot be fully realized. However, the metal loss also contributes to this problem, because the predicted 0.6 mm reduction in wall thickness after 100,000 h experienced in the field tests would result in an increase in stress of 12%. There are, however, exceptions to the 600 °C limitation for T91 and T92 type steels, as discussed earlier.

The principle conclusion from all of the above studies is that in laboratory tests, described above, the type of exposure did not matter as long as the environment contained moisture. Furthermore, though the corrosion behavior was similar, substantial differences occurred in the oxide morphology, and the scale exfoliation tendencies may vary accordingly.

3.4.3 Effect of Steam Pressure. Most of the experimental work on steam oxidation was done at steam pressures significantly lower than operational steam pressures, most at less than 1 atm (14.5 psig), whereas supercritical steam conditions would require higher pressure, greater than 218 atm (3208 psia). Watanabe et al. (Ref 30) reported only a small effect of pressure over the range 2-10 MPa. However, the activation energies reported from this work are much higher than those reported by others, suggesting that the rate controlling mechanisms might be different than at the lower pressures. From low-pressure studies in Ar-water vapor mixtures, Fujii and Meussner (Ref 13, 14) reported strong pressure dependence in the temperature range of 800-1100 °C (1472-2012 °F) with the oxidation rates increasing when the pressure was increased from 0.05 to 0.10 atm (0.73-1.46 psig).

Pearl et al. (Ref 50) showed that the mass loss of Alloy 625 in flowing superheated steam increased considerably with the temperature and exposure time. The mass loss of alloy due to corrosion by superheated steam also was observed (Ref 51, 52). Their results showed that the corrosion rate of austenitic stainless steel and high-Cr, high-Ni alloys increases with the steam temperature and pressure. A similar effect was also reported for SUS347HTB, 17-14CuMo, 20Cr-25Ni, and 22Cr-35Ni steels (Ref 52).

Kaano et al. (Ref 53) reported that in a low temperature range 570-600 °C (1058-1112 °F), steam pressure had an adverse effect on oxidation, and chemical composition had no effect on the oxidation rate. At a higher temperature range 620-700 °C (1148-1292 °F), the steam pressure effect was minor and the effect of chemical composition (Cr content) became dominant. Wright and Pint provided a listing of prior work that summarized the temperatures and pressures used in various steam oxidation studies since 1962 on alloys of potential interest (Ref 6). The table showed only two cases that correspond to supercritical conditions, but none of the test conditions replicate the highest temperatures and pressures that will be realized in an ultra-supercritical boiler.

Paterson, et al. (Ref 10) suggested that the oxide scale growth rate constant for ferritic boiler tube materials is proportional to $P^{1/5}$ (the bulk steam pressure to the 1/5th power). This relationship was derived from oxide thicknesses on superheater tubes that were 45% thicker than on reheater tubes. The tubes displayed the same temperature, but different steam pressures. The authors felt that the pressure effect was caused by differences in the partial pressure of oxygen.

In the subcritical region, it is considered that pressure has little effect. However, recent work on NF709 has indicated a relationship between oxidation rate and the square root of pressure (Ref 52). However, these results were for only 500 h exposures, and the effect was not as marked for type 347H steel. Even if these results indicate a real trend, the effect of pressure will not become significant in more advanced supercritical plants compared with currently operating supercritical plants because the pressure increases in the advanced plants planned in the short-to-medium term are not significantly higher than those of current supercritical units.

3.4.4 Effect of Pretreatments. Beneficial effects due to grain refining have been pursued as a proven method for improving oxidation resistance of austenitic steels. A typical example is 347 HFG, which has been applied widely in the grain refined condition and favorable service experience, up to 50,000 h has been experienced. Currently, the technique is being extended to other stainless steel such as SUPER304H. Grain refinement leads to more protective scale morphology. An example of scale morphology differences, and corresponding service experience is shown in Fig. 13 (Ref 58).

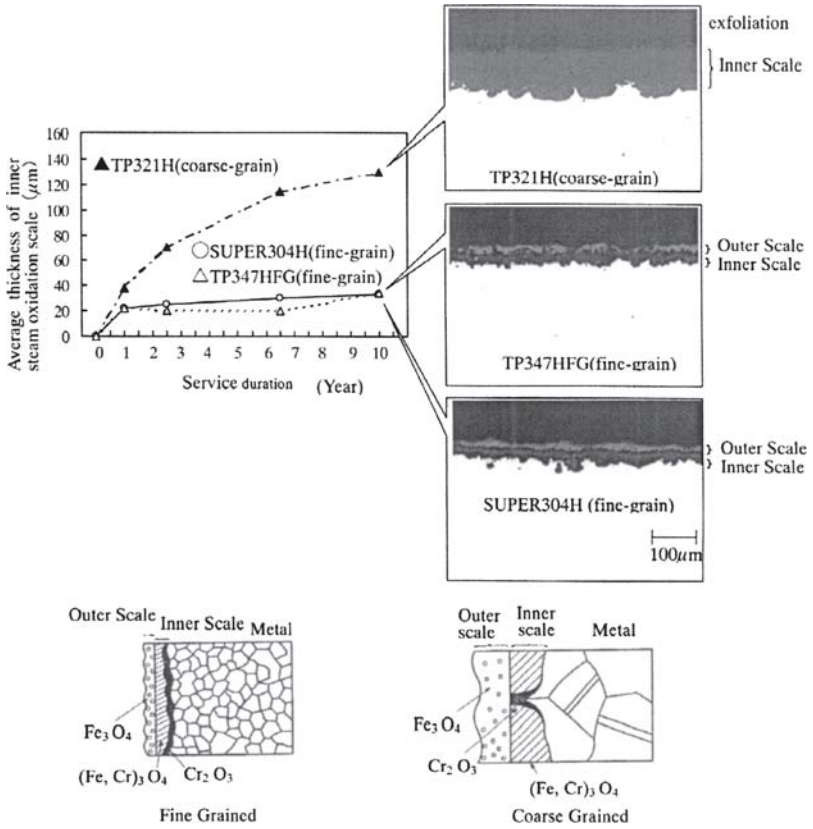

Fig. 13 Steam oxidation scale of fine-grained and coarse-grained 347H steels (Ref 58)

Surface pretreatments have been shown to affect the steam oxidation behavior of alloys. It causes structural changes and may influence the corrosion characteristics of materials (Ref 54-56). Experiments on alloys with ≥6.7% Cr showed an increase in corrosion resistance with increased cold work (Ref 57). For 80% cold deformed alloys containing more than 11% Cr, a gain of 70-75% in corrosion resistance (compared with the metal loss of the nondeformed material) occurred after 1000 h exposure. Microanalysis detected high Cr content at local areas of the highly deformed 18.7% Cr alloy following oxidation.

Sato et al. (Ref 33) have described substantial beneficial effects on oxidation resistance of austenitic stainless steels due to shot blasting. This technique has been applied to conventional austenitic steels in Japan, for more than 20 years. According to the authors, the shot blasted austenitic steels with 18-20% Cr can exhibit excellent oxidation resistance up to 700 °C (1300 °F) compared with HR3C containing 25% Cr. Thus, they claim that the shot blast technique enables SUPER304H to be used in 600 °C (1112 °F) class USC boilers. Long field experience time in many plants up to 50,000 h has confirmed the beneficial effects of shot blasting such that it has become routine practice, as stated by one boiler manufacturer (Ref 33). A combination of shot blasting and fine-grained 347 HFG and SUPER304 H steels produced oxidation resistance that was vastly superior to conventional stainless steels (Ref 58). The effect of shot blasting alone was lost above 700 °C (1300 °F). Shot-peened fine-grained steels retained their superiority above 700 °C due to the fine grain size. Hence, the combination of fine grain size and shot blasting was the most desirable (Ref 58). An example of Matsuo's results is shown in Fig. 14. The effect of grain refinement, combined with shot peening, was retained at temperatures above 700 °C (1300 °F). Preoxidation treatments have also been found to be beneficial in retaining oxidation (Ref 59).

The effect of cold work pretreatment on corrosion rate is explained by improved diffusivity of Cr in the defect structure, preferential oxidation, and formation of a solid solution ($FeFe_{2-x}Cr_xO_4$) spinel-type oxide scale. For cold-worked materials, protective Cr-rich oxide scales with low defect concentrations and reduced ion diffusivity were formed, which controlled the corrosion reaction. Thus, especially in the case of highly deformed materials with medium Cr content, the oxidation changed over from a parabolic to a logarithmic rate law.

4. Austenitic Steels and Ni-Base Alloys

Austenitic steels are used for thin section heat transfer tubing at temperatures above the metal temperature limit for ferritic steels. A comparison of the relative steam oxidation rates of ferritic and austenitic materials from tube sections exposed in the secondary superheater of a subcritical steam boiler at temperatures of 545 and 565 °C (1013 and 1049 °F), respectively, indicated approximate steam-side oxide thicknesses after 10,149 h of 105 and 60 μm (4.1 and 2.4 mil) for the ferritic materials NF 616 and HCM12, respectively, and approximately 40-50, 30, and 20-25 μm (1.6-2, 1.1, and 0.8-1.0 mil) for the austenitic materials SUPER304H, HR3C, and NF 709, respectively (Ref 49). Field results from other power stations have also been reported in Ref 49.

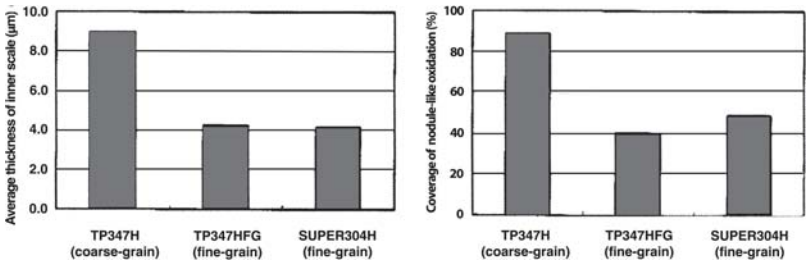

Fig. 14 Laboratory steam oxidation test results of shot-peened fine-grained and shot-peened coarse-grained austenitic stainless steel at 750 °C (Ref 58)

Yoshikawa (Ref 60) observed differences in the exfoliation characteristics of four commercial stainless steels identified as 304H, 321H, 316H, and 347H in a test loop at 650 °C (1202 °F), where 347H showed the least oxidation and 316H showed the most oxidation. Yoshikawa found that fine grains and increased Cr content reduced the oxidation. However, the oxidation rate increased rapidly with an increase in temperature between 625 and 650 °C (1157 and 1202 °F).

When several materials were tested at 532 °C (990 °F) for 1000 h (Ref 28), steels containing more than 20% Cr (Alloys 807, 800H, and HR3C) and fine-grained 347H displayed better scaling resistance than the conventional coarse-grained and lean austenitic stainless steels. The steel containing the highest Cr concentration in this study (HR3C with 24% Cr) displayed almost no scale formation. A clear trend was observed between the Cr concentration and the scale thickness in this program. Similarly, in supercritical steam of 538 °C (1000 °F) and 24.5 MPa for 5000 h, the mass gain for 347 SS (18% Cr) and Alloy 800 (21% Cr) was 1.5 and 0.9 mg/cm^2, respectively. The Ni-based alloys in this study [Alloy 600 (15.5% Cr; 0.5 mg/cm^2 mass gain), Alloy 718 (19% Cr; 0.015 mg/cm^2 mass gain) and Alloy X (22% Cr; 0.08 mg/cm^2 mass gain)] performed even better, but the correlation between mass gain and Cr content was not obvious.

Nickel-base alloys are frequently selected for their superior corrosion resistance to supercritical and high-temperature steam. Alloy 718 exhibited (Ref 56) a mass gain of 0.01 mg/cm^2 at 538 °C (1000 °F) after 10,000 h (Ref 56). Very little or no scale was observed on Alloy 617, Alloy 625, Alloy X, and SZ alloy (Ref 61) when exposed to 700 °C (1292 °F) steam for 1000 h. Early work by Pearl (Ref 62) also indicated that the corrosion rates of Ni-rich, Ni-base alloys in superheated steam are lower than that of the Fe-rich, Ni-base alloys, Alloy X, and 304 SS. The alloys with high Cr had excellent scaling resistance to high temperature and supercritical steam containing oxygen.

Long-term exposure of these fine grain steels for up to 10 years to high-temperature steam used as superheater and reheater tubings in a practical 1060 °F boiler were proved successful (Ref 58). Again, the growth of oxide scale on these fine grain steels was minimal after exposure of one year, although oxide scale on coarse grain TP321H steel continued to grow according to the parabolic rate law. The effect of grain size on scaling has also been described by Nishiyama et al. (Ref 63).

The oxidation rate of austenitic stainless steels in high temperature steam becomes drastically reduced for steels and alloys of high-Cr, high-Ni system, e.g., more than 25% Cr (Ref 64) and is attributed to the uniform formation of protective Cr_2O_3 scale for 25%Cr steels, not at the inner scale-base metal interface as in 18% Cr fine grain steels, but at the surface of the boiler tubes.

The beneficial effect of Ni in combination with Cr in austenitic steels and Ni-base alloys has been confirmed by Otoguro et al. (Ref 64) and Osgerby and Fry (Ref 37). The latter proposed a Cr equivalent for Ni-base alloys with beneficial effects from Cr, Mn, Mo, and W, and negative correlation with Co. Oxidation rates appeared to be relatively unaffected by alloy strengthening additions such as Mo, Ti, and Nb for steels containing more than 20% Cr (Ref 64).

Compared with ferritics, the amount of data for austenitics and Ni-base alloys is small. More data pertain to SUPER304H, 347HFG, and 321 SS because these grades are commonly in use. These studies include those by Sato et al. (Ref 33) on shot peened SUPER304H; Matsuo et al. on 321SS, 347HFG, and SUPER304H, both in the laboratory and in the field (Ref 58); Masuyama et al. (Ref 65) on chromized 347, 347HFG, 17-14CuMo; and Tempaloy (Ref 58). Much of the available data is described in the section 3.4.4 on surface treatment effects and in a later section 8 on alloy selection.

5. Oxidation Mechanism

The composition and structure of scales forming on Fe-Cr alloys depends on the amount of Cr in the metal, on temperature, time, other alloying elements, heat flux, grain size, etc. Steam oxidizes steel because the partial pressure of oxygen generated by dissociation of steam ($2H_2O = 2H_2 + O_2$) is higher than the oxygen pressure produced due to the dissociation of iron oxides and of the oxides of most alloying elements.

Effertz and Meisel (Ref 66) have described the mechanism of scale formation in which oxygen molecules, produced by dissociation of steam, are adsorbed on the surface of an oxide, which is always present on steel under normal conditions. The next step involves dissociation of the oxygen molecules, ionization of oxygen atoms to oxygen ions, and chemisorption of the oxygen ions. The necessary electrons are provided by the metal and are transported by diffusion through the oxide layer to the oxide/steam interface. The chemisorbed oxygen ions are incorporated in the spinel lattice forming a new layer of magnetite with a high concentration of metal defects. At the metal-oxide interface, metal ions and electrons are transferred from the metal lattice into the scale and occupy interstitial positions in the spinel lattice of magnetite. Oxygen ions from the scale enter the uppermost layers of the Fe lattice and start to form a spinel lattice. In this way, two layers of scale are growing from the original metal surface: one is growing outward and the other inward. Both consist of spinel, but the outer layer is rich in Fe vacant sites, while the inner one is characterized by Fe excess and oxygen vacant sites. The inner layer also contains most of the alloying elements from the steel. The boundary between the inner and outer layer, representing the original

position of the steel surface, is usually porous because diffusion along vacant sites (outer scale) is faster than diffusion along interstitial sites (inner scale).

A common finding in many of the studies of oxidation in steam or water vapor is that the scales exhibit significant porosity, to the extent that the suggested oxidation mechanisms invoke transport of Fe out and steam in via an interconnected pore network. Surman and Castle (Ref 67) suggested that Fe was transported in the vapor phase [via the volatile species $Fe(OH)_2$] through pores and cavities from the metal-oxide interface to the outer layer. However, Cory and Herrington (Ref 68) pointed out that Co and Ni hydroxides have similar volatilities and remained in the inner layer. Mayer and Manolescu (Ref 69) agreed with Surman and Castle (Ref 67) on the importance of vapor-phase transport and considered two possible mechanisms may operate: vapor-phase transport, or provision for the growth of the inner layer by dissociation of the outer layer.

6. Oxide Scale Morphology

It is useful to know the types of oxide scales that are likely to form in the environment as a function of metal temperature and steam pressure. Figure 1 provides a summary of the salient features of scale formation in steels as a function of Cr content.

It is well-known C steel forms two oxides: magnetite (Fe_3O_4), as an inner layer, and hematite (Fe_2O_3) at the gas interface at temperatures up to approximately 550 °C (1022 °F) (Ref 5). The composition of scale growing on Fe in air is similar to that produced in steam. At higher temperatures wustite (FeO) is formed at the metal-scale interface. The main difference in the composition of the higher temperature scale is that wustite forms at a lower temperature [560 °C (1040 °F)] when exposed to steam than in air. The presence of wustite in the steam-formed scale leads to an increase in the oxidation rate as compared with oxidation in air (Ref 18). Davies et al. (Ref 70) have measured the growth rate of wustite to be about 10 times greater than that of magnetite. At 700 °C (1292 °F), the scale on Fe exposed to steam consists entirely of wustite according to Heindelhofer and Larsen (Ref 71).

Wustite is the least protective of the three oxides because it has the highest diffusion coefficient for the Fe ion due to its high concentration of vacant Fe lattice sites in the crystal structure (Ref 18). Magnetite, with its spinel structure, is also cation-deficient, but to a much lesser degree than wustite, so that it represents a more protective scale. The best protective properties have been observed with hematite, but this oxide forms only a very thin outer layer and has little effect on the oxidation rate.

With respect to low Cr alloy steels (0-3% Cr), the following scenario occurs. At steam temperatures below 580 °C (1076 °F), the scales formed on the lower Cr alloys consist of magnetite and are initially double-layered. With increasing time (8000-10,000 h), multilayered scales develop and there is some indication that spallation of some of these layers may occur. Mayer and Manolescu (Ref 69) described the formation of double-layered scales on dilute Fe-Cr alloys in steam. They observed an outer layer of magnetite characterized by a columnar grain structure with pores at grain boundary triple points, an inner layer of magnetite with an equiaxed grain structure with irregular porosity (apparently in rows parallel to surface), and a Fe-Cr spinel at the metal surface. The ratio of the thicknesses of the inner and outer layers was independent of time but increased with increasing alloy Cr content.

There are two types of oxides that can develop on steels containing higher levels (up to 12%Cr) of Cr (Ref 72). One is basically chromium oxide (Cr_2O_3) with a rhomohedral lattice and excellent protective properties. The other Cr-based oxide is a spinel $(Fe,Cr)_3O_4$, which is less protective compared with Cr_2O_3. Only in the inner spinel layer is Cr present in amounts that exceed the Cr concentration in the steel. Chromium oxide forms solid solutions with hematite, and a mixed oxide $(Fe,Cr)_2O_3$ is usually observed when this type of scale evolves. In the spinel, Cr substitutes for trivalent Fe so that the compositions range from pure magnetite with zero Cr to the spinel $(Fe,Cr)_3O_4$ with about 46% Cr. The presence of Cr in the spinel reduces the diffusion coefficients of metallic ions through the inner spinel lattice by reducing the number of vacant sites and by increasing the energy of the diffusion jumps, resulting in lower oxidation rates.

Cory and Herrington (Ref 68) reported that both layers of the two-layered scales formed on Fe-2.25Cr and Fe-9Cr alloys were magnetite, and the interface between the layers corresponded to the original metal surface. The scales had a laminated appearance, which had also been seen by Hurst and Cowan (Ref 73), with alternating bands of dense and porous scale, suggestive of formation by plastic settlement and collapse. The scales were less porous than reported earlier (Ref 69), but the outer layer was more porous than the inner. On the Fe-9Cr alloy, internal oxidation along surface grain boundaries occurred. The depth of penetration was temperature-dependent. Itagaki et al. (Ref 41) reported the formation of a thin Cr-rich oxide, with no evidence of magnetite formation, on a 9% Cr-based alloy (NF616 with 3% Pd) in steam at 650 °C (1202 °F). Fakuda and Tamura (Ref 26) reported that in a 9Cr1Mo alloy, the outer layers are magnetite and inner layers are iron-chromium oxide (Fe-Cr spinel). In 9Cr1Mo0.8Si steel, a continuous Cr-rich layer was observed in the inner oxide at the scale–metal interface and a build up of Si was obviously observed in the Cr-rich layer. In 9Cr1Mo0.2Si steel, the accumulation of Si was not detected in the inner layer at the scale-metal interface and multiple Cr-rich layers were found dispersed in the inner scale. These findings suggest that an appropriate addition of Si could contribute to the formation and stability of a Cr-rich layer, which can sufficiently prevent the outward diffusion of Fe, consequently reducing the oxidation rate.

In a Fe-11Cr alloy, Zurek et al. (Ref 74) reported the formation of double-layer scale. Chromium depletion of up to 6 μm deep was observed in the base metal that was adjacent to the scale. This Cr was incorporated in the oxide film. At 900 °C (1652 °F), preferential formation of oxide along the metal grain boundaries was observed. With increasing temperature, however, this effect became negligible. The inner scale, consisting of wustite and spinel ($FeCr_2O_4$), was not uniform and homogeneous. Knodler and Ennis (Ref 75) also reported that alloys with 11-12% Cr displayed inhomogeneous scales with poorly reproducible thickness, whereas steels with <9% Cr show uniform and reproducible scale growth. Some porous regions are present within this region, and the scale morphology is complex. The amount of Cr is not sufficient for forming a protective layer of Cr_2O_3, and therefore, a double layer scale is actually produced on the steel surface. It appears that the protective behavior associated with the formation of a

continuousCr_2O_3 layer is not necessarily observed in steam at alloy Cr levels below approximately 20%.

Other authors reported that with increasing alloy Cr content in ferritic steels, a Cr-rich spinel phase, $Fe_{2-x}Cr_xO_4$, forms at the metal-oxide interface (Ref 53). The diffusion of cations through this spinel is significantly reduced, and the oxidation rate is slowed. At sufficiently high Cr levels (depending on temperature) the Cr content of this layer increases and eventually forms Cr_2O_3, which grows at an appreciably slower rate. Watanabe et al. (Ref 30) found that under all testing conditions [560 °C and 700 °C (1040 and 1292 °F); 10 and 99 atm (145 and 1450 psi) total pressure], duplex scales were formed on alloys containing 2% and 9-11% Cr. Both layers were basically magnetite; the outer layer was Cr-free, whereas the inner layer was enriched in Cr, which became more pronounced for the 9-11% Cr steels at the higher testing temperatures. The inner layer of the 11% Cr alloy exposed to 700 °C and 99 atm (1292 °F/1450 psig) steam contained over 40% Cr, which was considered to provide an effective diffusion barrier. While the maximum Cr contents of the inner layers on the 9-11% Cr steels increased with temperature, especially above 600 °C (1112 °F), 2% Cr steel exhibited a maximum Cr concentration in the inner layer of less than 13%. In both the higher-Cr alloys tested, a layer of internal oxide particles was observed beneath the inner oxide layer. Such layers were more apparent at the lower temperatures. There was no clear effect of Cr concentration on the parabolic oxidation rate constant at 570 and 620 °C (1058 and 1148 °F), but at 700 °C (1292 °F) there appeared to be an almost linear decrease in the rate constant with increasing Cr concentration. This decrease in the rate constant was apparently caused by the increasing maximum Cr content of the inner layer.

A laboratory study in Ar-0.1 water vapor suggested that the oxidation behavior was not controlled by diffusion through the scales (Ref 13). The strong pressure dependence of oxidation in Ar-water vapor mixtures, the low activation energy, and the peculiar scale morphologies were taken to indicate that the rate controlling process occurred at the gas-oxide interface and the rate of oxygen transport inwards is very slow. In contrast, a study under similar conditions in which iron oxide layers were formed represented the oxidation kinetics as parabolic (Ref 76).

Scales formed on austenitic 18Cr-8Ni steels are similar to those formed on ferritic steels (Ref 18). Two distinct layers of magnetite of about equal thickness are formed, but they are usually thin and contain less alloying elements in the inner magnetite layer. The oxides are predominantly spinel, the inner layer being rich in Cr (Ref 80). Otoguro and Tamura reported that the scales were composed of two layers, i.e., magnetite (outer scale) and spinel containing Cr and Ni and $(Cr,Fe)_2O_3$ (inner scale) (Ref 64). The Ni enriched layer is formed on the metal surface beneath the oxide which suppresses the scale growth (Ref 78). The specimens oxidized under a high steam pressure exhibited voids and cavities in the outer scale. These voids and cavities are attributed to the local cessation of the scale growth, difference in diffusion rate of metallic ions between the outer and inner scales, and/or weakening of the oxide grain boundaries. Linkage of these cavities can lead to spallation of the outer oxide scale.

Otsuka et al. (Ref 61) explained that once the Cr concentration of high-Cr, high-Ni steels and alloys exceeds ~25%, a Cr_2O_3 oxide forms directly on the metal surface instead of at the interface between the metal surface and a magnetite scale. This Cr_2O_3 oxide is very thin and leads to greatly reduced oxidation rates compared with steels containing ~18% Cr (304SS, 347SS, etc.).

In summary, scale composition changes from Fe_2O_3/Fe_3O_4 in simple low alloy steel to $Fe_3O_4/(Fe,Cr)_3O_4$ in 9-12% Cr steels to $Fe_3O_4/(Fe,Cr)_3O_4/Cr_2O_3$ in 18-8 type stainless steels to Cr_2O_3 in stainless steels containing >25% Cr, in increasing merit of protection. The first species in each case is the layer at the gaseous interface and the last species is the layer in contact with the metal.

7. Exfoliation

It is known that exfoliation of oxide scales is primarily associated with the stress in the scale (Ref 79). It is expected that the volume increase of the growing scale itself produces stresses in the scale as well as at the metal-scale interface. In addition, difference in thermal expansion between the scale and the substrate also serves as a source of stress under cyclic operation. The latter source of stress has been identified by a number of researchers as being significant to the magnitude of strain acting on the scale when it is cooled (Ref 80, 81). It has been noted that T23 alloy containing W may spall more readily than T22 due to the higher creep strength of T23 resulting in less relaxation of stresses developing during cooling (Ref 82).

Scale structure can affect the ability of the scales to withstand strains. Voids can create planes of weakness within the scale or at the metal-scale interface. The outer magnetite layer tends to be porous, and voids are often observed between the inner Cr-rich spinel layer and the outer layer (Ref 18). Some of these voids are probably formed by condensation of vacancies created at the metal surface during transfer of metal atoms from the metal lattice into the oxide lattice (Ref 83, 84). In many instances, the exfoliated scales are two-layered suggesting that separation is at the metal-scale interface. Exfoliation occurs in some cases near the metal-scale interface and in other cases at the interface between the outer and inner part of the scale (Ref 22). The different exfoliation mechanisms seem to be related to differences in coalescence of pores present in the scales. Exfoliation, or spalling, is the final separation step in a series of events, which may have started with crack initiation at pores or defects. At higher steam temperature, exfoliation becomes more severe with each incremental temperature increase. The tube wall thinning caused by exfoliation is not as serious in most cases as the damage caused by the detachable scale, which may result in plugging as well as inevitable turbine erosion.

It has been noted that voids are frequently found in scales formed in power plants but that scales grown in the laboratory contain few voids. The oxides formed isothermally on specimens have been reported to contain few voids until after many thousands of hours, usually not until spalling was about to begin, and then numerous voids were apparent. On the other hand, experiments conducted with 2-1/4Cr-1Mo steel in which a high heat flux existed across the corroding surfaces have shown numerous voids even in the early stages of oxidation (Ref 14, 15). Furthermore, oxides formed under these conditions appear to be much less firmly anchored to the substrate than those in isothermal tests. Comparison of isothermal results with those obtained with a high heat flux across the corroding surface suggests that under otherwise similar conditions, a high heat flux produces in a short time the same type of oxide

degradation that occurs only after much longer times without heat flux. The voided scales formed in service are inherently weaker and more susceptible to spalling than scales formed isothermally. These postulates have also been supported by Griess et al. (Ref 44). In comparing spallation tendencies, the exposure environment should also be kept in mind, because as discussed earlier, it can have a significant effect on the scale.

Exfoliation is common to both ferritic alloys and austenitic stainless steels, although stainless steel forms a thinner scale. Only full cool-down and warm-up cycles generated exfoliation from ferritic steel (such as T22), whereas stainless steels exfoliated while cooling down, release smaller particles than the ferritic steels. Even this thin scale is often very abrasive to the downstream steam turbine. Surface modification demonstrated reduced scale growth and exfoliation as mentioned earlier.

The scale-exfoliation problem with current steam generator and superheater tube materials intensifies hyperbolically (Ref 79) rather than linearly with increased temperature. Scaling data of ferritic alloys of up to 9% Cr indicated a rapid rise in corrosion rate where wustite (FeO) formed at the metal interface (Ref 79). It was observed that increasing the temperature from 538-566 °C (1000-1050 °F) nearly doubled the scale thickness in long-term exposures. The scale growth rate is controlled by the oxide phase rather than by the alloy content of the steel. Wustite formed above 595 °C (1103 °F) weakens the metal-oxide bond and promotes the formation of cracks and voids. A substantial reduction of scale growth and resistance to exfoliation was obtained by using an aqueous chromate treatment at elevated temperature and pressure (Ref 79). The chromate pretreatment resulted in a scale containing an Fe-Cr spinel at the midband of the scale. This Fe-Cr spinel phase suppresses the wustite formation at the scale-metal interface.

Hematite, which is often found on the outer surface of the two-layer magnetite scale, has a much lower expansion coefficient than magnetite in the range of 500-550 °C (932-1022 °F) and thus is prone to spalling (Ref 80). The Cr content of the scales, which is primarily a function of the alloy, also affects the thermal expansion coefficient and thus the cooling thermal strains between the inner and outer magnetite layers. Another factor that plays a role in exfoliation is the curved surface inside the tubes because scales growing on highly curved surfaces of small diameter tubes will be more adherent.

Experience with the higher Cr austenitic alloys (types 304, 316, 321, and 347 steels) has shown they exhibit slower oxidation rates than the low-Cr ferritic alloys due to the formation of more protective (Cr-containing) scales (Ref 5). Though scale exfoliation also occurs, it is to a lesser extent and only the outer magnetite layer is lost. As a result, the overall oxidation rate of these alloys in steam is closer to parabolic than linear. The annealed and pickled stainless steels are subject to greater exfoliation than the nonannealed (or shot-peened finish) due to surface Cr depletion (Ref 79). No exfoliation was observed in 9-11% Cr steels such as Sandvik HT-9, 9Cr-1Mo with 0.46% Si, and Sumitomo 9Cr-2Mo steels, when exposed to 482-538 °C (900-1000 °F) for up to 28,000 h (Ref 29). Knodler and Ennis (Ref 75) found that alloy NF616/P92 exhibited parabolic oxidation for times up to 1500 h at 650 °C (1202 °F) in 1 atm (14.5 psig) steam, after which scale spallation led to a deviation from parabolic. Models have been developed that predict the critical temperature drop required to initiate spallation (Ref 79).

The oxidation behavior of Alloy 825 in steam was studied between 600 and 1000 °C (1112 and 1832 °F) from 2 min to 100 h (Ref 85). The oxide scale remained adherent with no spalling or dimensional changes.

8. Selection of Alloys

Selection of materials for high-temperature applications is governed by a number of factors such as creep strength, steamside oxidation resistance, fireside corrosion resistance, weldability, fabricability, etc. The properties that are used by boiler designers to set upper limits for use of materials are creep (rupture) strength and fireside corrosion. The steamside corrosion rates are of interest primarily from a component longevity point of view. Even with respect to steamside oxidation, distinction has to be made between components operating under heat flux conditions versus those that run isothermally. For instance, headers, steam pipes, and penthouse tubes operate isothermally, and the metal temperature and the steam temperature in these components are the same. In heat transfer tubes, however, a thermal gradient is present. Tube temperatures can often exceed the steam temperature by as much as 50 °C, and in addition, the tube temperature increases with time due to the buildup of scale. The design temperature for a superheater is typically 35 °C (63 °F) higher than the rated steam temperature. One has to treat creep life under a changing scenario of oxide morphologies, oxidation rates, and temperature. In addition, the stress increase caused by wall thinning from fireside and steamside corrosion has to be taken into account. The life of these tubes has to be computed under continuously increasing stress and temperature conditions. Several computer codes are available in industry to perform such calculations. These types of calculations are needed to set allowable temperatures and stresses for heat transfer components. Hence, for the same alloy, the allowable temperature limit for a header may be higher than for a superheater tube. Because design stresses from the creep rupture point of view do not account for environmental effects, temperature limits based on creep rupture consideration alone are likely to be nonconservative and will represent the upper limits.

Based on results of various references cited earlier and from three-year field tests by Masuyama (Ref 86), alloys can be ranked as (HCM12, 347HFG), 321H and 9Cr steels. Masuyama claims HCM12 to be equivalent to 347HFG and vastly superior to 321H and 9Cr steels. Masuyama et al. also suggest that the HCM12 alloy will have less exfoliation tendency. Table 4 summarizes oxide thickness measured on the steamside of a range of steels exposed to plant trials. Both steam and metal temperatures are indicated. The general indication appears to be that, as tube temperature rises toward 700 °C (1292 °F), enhanced versions of the austenitic steels such as NF709, HR3C, AC66, and HR6W will be needed to minimize the boreside oxide film thicknesses.

Material selection from a creep point of view is generally based on failure in 100,000 h at a stress of 100 MPa at the temperature of interest. The allowable temperatures listed in Table 1 are purely based on this type of consideration. Steamside oxidation can reduce these limits by another 35 °C for heat transfer tubing. For nonheat transfer components such as headers and piping, the temperature limits can be identical to the creep based temperatures listed in Table 1. For instance, the T92 alloy may be usable for headers up to 620 °C, but only up to 585 °C for superheater tubes. Another consideration that affects material selection is coal ash corrosion. If external cor-

Table 4 Steam-side oxide thicknesses measured in plant trials

Alloy	Cr, %	Power plant	Steam T (metal T), °C	Exposure time, h	Oxide thickness, μm
T91	8-9.5	Wilhelmshaven	600-605 (621-636)	11,000	330
E911	8.5-9.5	Wilhelmshaven	600-605 (621-636)	11,000	460
NF616	8.5-9.5	Mizushima 2	(545)	10,149	105
NF616	8.5-9.5	Wilhelmshaven	600-605 (621-636)	11,000	325
HCM12	11-13	Mizushima 2	(545)	10,149	60
Esshete 1250	14-16	Wilhelmshaven	600	12,463	40-80
Esshete 1250	14-16	North Wilford	(660)	12,719	100-148
Esshete 1250	14-16	Skelton Grange	(633-677)	6,840	200-230
1.4910	…	Wilhelmshaven	600	12,463	909-120
Super 304H	17-19	Mizushima 2	(565)	10,149	40-50
NF709	19-22	Mizushima 2	(565)	10,149	20-25
HR3C	24-26	Mizushima 2	(565)	10,149	30
AC66	26-28	Wilhelmshaven	600	12,463	Negligible

Source: Ref 49

rosion is a serious consideration, use of very high Cr coatings or claddings may become necessary even for Ni-base alloys and austenitic steels.

There is some disagreement regarding the upper limit of temperature for T91 and T92 9% Cr alloys. The works of Fleming et al. (Ref 49) and Ennis et al. (Ref 48) were cited as limiting the temperature of use to 600 °C. Though this statement may be true for thin superheater tubes, it does not apply to certain categories of thick walled tubes used in certain designs and to heavy section piping and headers. For these applications, the temperature, from a steamside oxidation point of view, can be pushed up to 629 °C (1150 °F). Unfortunately, very little data is available on Ni-base alloys of interest, such as IN740, Haynes 230, Marco Alloy 617, HR6W, etc. Based on the Cr content, it is estimated that these alloys will be at least as good as the best high Cr stainless steel, such as HR3C. Based on current knowledge, these alloys can be ranked in decreasing order of oxidation resistance: (IN740, Haynes 230, Marco alloy, HR6W), (HR3C, NF709, IN625, IN617), IN800H, (347H, SUPER304H fine grained), (HCM12A, HCM12), 321H, (NF616, T91), and (T22, T23). Alloys listed within parenthesis are expected to be comparable in their performance.

The effects caused by surface treatments cannot also be overlooked. The substantial benefits from grain refinement, shot-peening, and their combination thereof, have already been discussed. It is believed that these treatments may make 18% Cr steels competitive with respect to alloys of much higher Cr content (25%), in terms of oxidation resistance. Ultimately, economics will dictate choice of the materials.

9. Field Studies

It was already discussed that laboratory studies invariably do not simulate the behavior of alloys in actual boilers, and that the oxide morphologies and attendant spallation tendencies are different. By and large, laboratory studies are used primarily to rank alloys and study the effect of individual parameters on performance. Very little prediction can be made regarding the wastage rate from oxidation in the boiler. The field studies that have been cited include those by Fleming et al. (Ref 49), Masuyama et al. (Ref 58), Sato et al. (Ref 33), and Nishiyama et al. (Ref 63). Due to many differences between the studies, the data could not be consolidated. However, they fall within the scatter bands for different classes of materials, as cited by Osgerby and Fry (Ref 46). These results are presented in Fig. 15.

10. Recent Studies

As part of a national US study, steamside oxidation evaluations are being carried out on a variety of ferritic and austenitic steels and Ni-base alloys. These studies are designed to determine the steamside oxidation behavior and temperature limits of commercially available ferritic materials, austenitic stainless steels, and Ni-based alloys and to collect available literature on the steamside oxidation of these materials and to increase our understanding of the mechanism of steamside oxidation and the effect of variables such as alloying content and environmental conditions (Ref 87). The steamside oxidation tests are being performed on coupons in slowly flowing atmospheric pressure steam. The total exposure time at each temperature will be 4000 h, with interim specimen removals after 1000 and 2000 h. The test environment is high-purity water with 20-70 ppb ammonia to maintain a pH of 8.0-8.5 and 100-300 ppb dissolved oxygen. The specimens are coupons hung from a test frame and oriented parallel to the flow of steam. One coupon from each material was sectioned and metallographically examined with a scanning electron microscope equipped with energy dispersive x-ray analysis capabilities (SEM/EDX) to determine oxide morphology and composition. The other coupon for each material was de-scaled and weighed to determine the de-scaled mass loss experienced.

Steamside oxidation testing has been completed at 650 °C (1200 °F) for durations up to 4000 h (Ref 87). Test results show that among the ferritic steels, two new steels, MARB2 (9% Cr alloy developed by the National Institute for Materials Science [NIMS], Japan) and VM12 (developed by V&M Tubes, France) display the best oxidation behavior and all other 2-9% Cr steels exhibit severe oxidation. The chromized P92 steel appeared to perform better than the uncoated ferritic steels, but not as good as the austenitic steels. Ferritic steels that exhibit the lowest mass loss also exhibited the lowest tendency to spall. Clear evidence of spallation is observed in T23, T91, and T92. Other ferritic steels had much better resistance to spallation. No spallation is observed in the austenitic steels or Ni-base alloys in the 650 °C (1200 °F) tests. Of the austenitic and Ni-based alloys, the Co-containing ones, i.e., CCA 617, 740, and Nimonic 263, exhibited the best oxidation behavior in the

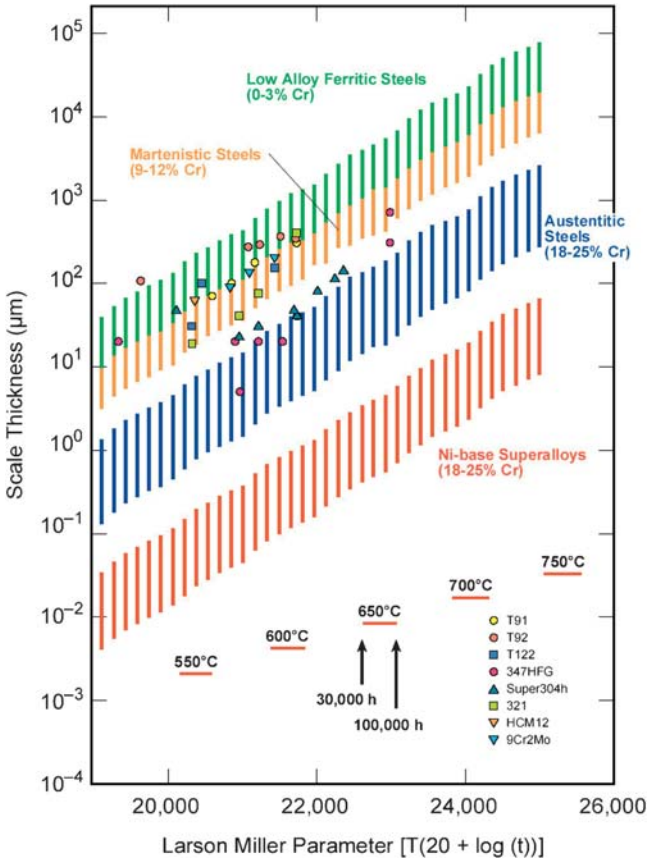

Fig. 15 Scale thickness increase with temperature and time expressed in terms of Larson Miller plot. Adapted from Ref 46

order listed. The results also indicate that at 650 °C (1200 °F), the austenitic and Ni-based alloys formed a dense Cr oxide that led to low oxidation rates. The oxidation of the alloys primarily followed parabolic kinetics. The rate constants calculated from the tests at 650 °C (1200 °F) are illustrated in Fig. 16 (Ref 89).

Steamside oxidation testing has also been performed at 800 °C (1475 °F) for up to 1000 h on 20 different ferritic, austenitic, and Ni-based alloys and coated materials. Results from the test program are shown in Fig. 17 (Ref 88). The data indicate that the oxidation susceptibility is independent of Cr level, once a threshold level of about 10% is reached. Among the Ni-base alloys, CCA 617, IN 740, Nimonic 230, HR 120, and HR 6W, showed oxidation resistance in decreasing order listed. The ferritic steel VM12 performed as well as some austenitic steels and Ni-base alloys. As expected, all alloys experienced greater oxidation at 800 °C (1475 °F) than at 650° (1200 °F). Austenitic alloy 214 (which contains ~4.5% Al) exhibited the lowest amount of oxidation and was found to have formed a dense Al oxide scale during exposure. Nickel-base alloys containing between 0.5 and 1.3% Al displayed near-surface intergranular Al oxide penetrations. Ferritic steel MARB2 and austenitic steel 304H formed oxide islands, indicative of the development of a nonprotective oxide. The predominant tendency among the austenitic steels for scale exfoliation was found in 347HFG, followed by 304H and SAVE 25. None of the other ausenitic and Ni-based alloys showed evidence of oxide spalling. Among the diffusion coatings applied in this research, SiCr and FeCr coatings performed much better than the Al-Cr coatings.

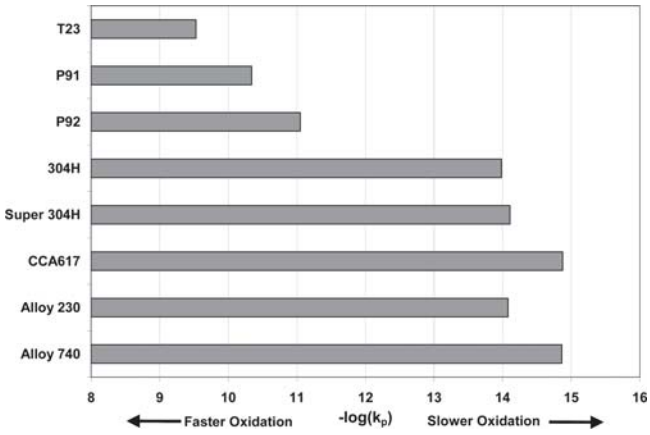

Fig. 16 Steam oxidation rate contants for various boiler steels (Ref 88)

11. Conclusions

Low alloy ferritic steels containing Cr in the range 0-3% obey a parabolic oxidation rate law below the temperature for FeO (wustite) formation. Above this temperature linear kinetics starts to develop until finally, with the dominance of FeO, the kinetics become completely linear. This crossover temperature may be decreased by steam and heat flux, and is increased by Cr content of the alloy. Cyclic operation of plant resulting in periodic spalling of scale can also be a factor in the transition from parabolic to linear kinetics. The crossover temperature cannot, therefore, be precisely defined. Short term isothermal tests in air or in steam are not necessarily representative of the real conditions in SH/RH tubes in a boiler. It is estimated that deviation from parabolic behavior may start at temperatures as low as 580 °C (1075 °F) and may not be completed until 700 °C in low alloy steels. The need to conduct realistic tests that simulate service conditions cannot be overemphasized.

All studies on 9-12% Cr ferritic-martensitic steels conducted in the range 600-700 °C show parabolic oxidation kinetics, regardless of the variables cited above.

Among the ferritic steels containing 1-12% Cr, steamside oxidation appears to be relatively independent of the Cr concentration up to 600 °C but is a function of the Cr concentration at temperatures above 600 °C. The 9% Cr and 12% Cr steels show similar oxidation rates at 600 °C, but at 650 °C, the 12% Cr steel displays better steamside oxidation resistance than 9% Cr steels in thick walled superheater tubing, in heavy section piping and headers, and in nonheat flux conditions. The high strength 9% Cr steels may be used up to 620 °C. Great care, however, should be exercised when selecting a 9% Cr steel for applications where metal temperatures will exceed ~600 °C.

In line with the conclusion above, the activation energy (and the rate constant) are nearly independent of Cr level up to about 600 °C but diverge widely above 600 °C depending on the Cr level. The Q values for 12% Cr steels become significantly lower than 9% Cr steels above 600 °C. The Q drops precipitously between 9 and 12% Cr. For this reason, Cr contents of at least 11% must be met, in specifying T122 alloy.

For all classes of alloys (ferritic, austenitic, and Ni-base alloys) investigated, the oxidation decreases up to about 12% Cr and then tends to level off at higher values of Cr. Beneficial results have been reported in ferritic steels containing 9-12%

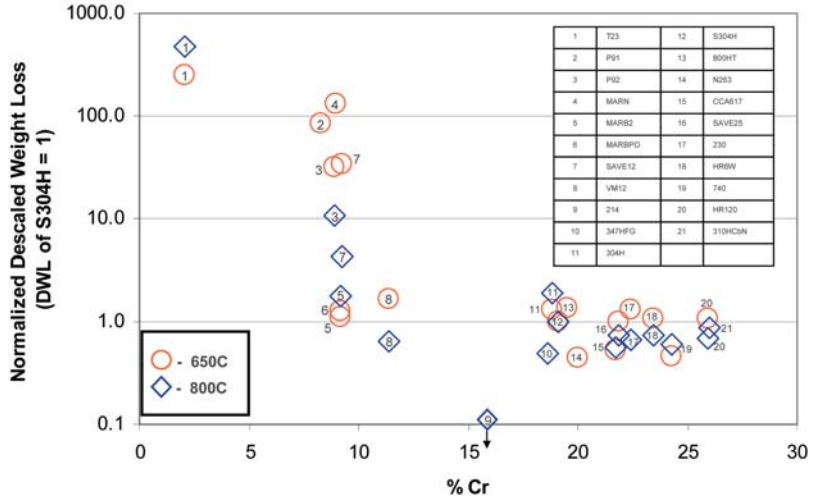

Fig. 17 Normalized weight loss due to steam oxidation for 1000 h at 650 and 800 °C (Ref 87)

Cr, because of alloy additions of Si, Pd, S, Mn, W, and Mo in restricted amounts, in terms of resistance to steamside oxidation. Sulfur levels of 50-100 ppm, Si levels of about 0.3%, and Pd levels of 3% are claimed to be optimal.

Tests conducted in steam under heat flux conditions are more severe than those conducted isothermally. The change from parabolic to linear kinetics often observed in boiler furnace tubes could well be the result of a temperature increase under heat flux conditions. The oxides formed under heat flux conditions are also believed to be less protective, more porous, and weaker under exfoliation conditions. Considerable care must be exercised in applying laboratory data to predict behavior of tubes in a boiler.

Chromizing and diffusion coatings Si-Cr, Fe-Cr, and Al-Cr are effective in reducing steamside oxidation, in decreasing order as listed.

The meager data available in the literature indicates that steam and air containing water vapor and simulated flue gases lead to higher rates of oxidation than dry air environments. Oxidation rates in steam and in flue gases were comparable because the latter contained steam, which predominated in its effect on oxidation. Accordingly, the oxide scale formed in steam has been found to be thicker, have more porosity than that in air, and contain external spinels $(Fe,Cr)_2O_3$ and $(Fe,Cr,Mn)_3O_4$ as opposed to Fe_3O_4 as the external scale in air.

The above result suggests that in the absence of coal ash corrosion, oxidation rates on the steamside and on the fireside of furnace tubing may be the same.

Though limited data exist showing that the increased pressure of steam may have an adverse effect on oxidation, the effects are believed to be minor and negligible.

With increasing Cr content, the scale morphology changes from Fe_2O_3 /Fe_3O_4 to Fe_3O_4/$(Fe,Cr)_3O_4$ to Fe_3O_4/$(Fe,Cr)_3O_4$/Cr_2O_3 to a pure Cr_2, O_3 layer, correspondingly, offering increasing protection.

Cold work and shot peening increase the oxidation resistance of ferritic and austenitic alloys. Shot peening combined with grain refinement produces even greater benefit in 304H and 347HFG. In this condition, the oxidation resistance is nearly equivalent to high Cr (25% Cr) steels, thus providing an economic alternative. These techniques are being increasingly applied to boiler tubes.

Available field data are full of scatter due to the many variables that affect oxidation. The data, however, can be fitted to a Larson-Miller type parameter approach that is consistent with previously published plots.

The ranking of alloys in decreasing order of oxidation resistance is CCA617, IN740, Alloy 230, HR120, HR6W, HR3C, NC709, 347HFG, SAVE25, Super 304H, VM12, SAVE12, T92, T91, and T23.

References

1. R. Viswanathan and W. Bakker, Materials for Ultrasupercritical Coal Power Plants – Boiler Materials: Part 1, *J. Mater. Eng. Perf.,* 2001, **10**(1), p 81-95
2. A. Hughes, B. Dooley, and S. Paterson, Oxide Exfoliation of 347HFG in High Temperature Boilers, 7th International Conference and Exhibition on Operating Pressure Equipment, April 2-4, 2003 (Sidney, Australia)
3. J.I. Wright, S. Paterson, and R. Dooley, Oxidation and Exfoliation, *EPRI Conference on Advances In Materials Technology for Fossil Power Plants,* October 2004, Hilton Head Island, SC, R. Viswanathan, D.W. Gandy, and K. Coleman, Ed., ASM International, 2004, p 370
4. R. Viswanathan, R. Purgert, and U. Rao, Materials for Ultrasupercritical Coal Power Plants in Materials for Advanced Power Engineering, *Proceedings of the 7th Liego COST Conference,* Lacomte-Beckerg, M. Carson, F. Schubert, and P.J. Ennis, Ed., 2002, Vol. 21, Part II, p 1109-1116
5. M. Staubli, K.H. Mayer, T.U. Kern, R.W. Vanstone, R. Hanus, J. Stief, and K.H. Schonfeld, Power Generation in the 21st Century, *3rd EPRI Conference on Advance in Materials Technologies for Fossil Power Plants,* March 21, 1981, Institute of Materials, 2001, U.K., p 15
6. I.G. Wright and B.A. Pint, "An Assessment of the High-Temperature Oxidation Behavior of Fe-Cr Steels in Water Vapor and Steam," Paper 02377 presented at *NACE CORROSION 2002,* April, 2002 (Denver, CO)
7. R. Viswanathan, *Damage Mechanisms and Life Assessment of High Temperature Components,* ASM International, 1987, p 229
8. S.R. Paterson, R. Moser, and T.R. Rettig, *Proc. International Conference on Interaction of Iron-Based Materials with Water and Steam,* R.B. Dooley and A. Bursik, Ed., EPRI Report No. TR-102101, 1992, p 8.1-8.5
9. I.M. Rehn and W. Apblett, "Corrosion Problems in Coal Fired Fossil Boiler Superheater and Reheater Tubes," Report CS-1811, Electric Power Research Institute, 1981
10. S.R. Paterson and T.W. Rettig, "Remaining Life Estimation of Boiler Pressure Parts – 2-1/4Cr-1Mo Superheater and Reheater Tubes," Project RP2253-5, Final Report, Electric Power Research Institute, 1987
11. M. Dewitte and J. Stubbe, Personal communication to D.A. Roberts of G.A. Technologies from Laboretec Company, Belgium, 1986
12. D.I. Roberts, Magnetic Oxide Thickness Time-Temperature Models

for 2-1/4Cr-1Mo Operating in High Pressure Steam, Letter to S. Paterson from D.I. Roberts, G.A. Technologies, San Diego, CA, 1986
13. C.T. Fujii and R.A. Meussner, Oxide Structure Produced on Iron-Chromium Alloys by a Dissociative Mechanism, *J. Electrochem. Soc.,* 1963, **110**(12), p 1195-1204
14. C.T. Fujii and R.A. Meussner, The Mechanism of High Temperature Oxidation of Iron Chromium Alloys, *J. Electrochem. Soc.,* 1964, **111**(11), p 1215-1221
15. P.H. Effertz and H. Meisel, *Der Machinenschaden,* (Damage to Machinery), 1971, **44**(1), p 14
16. M.L. Manning and E. Metcalfe, Scale Formations on Superheater Alloys, *Proceedings of International Conference on Ferritic Steels for Fast Reactor Steam Generators* (London), G.E. Lien, Ed., May 30-June 2, 1977, British Nuclear Energy Society, London, U.K., 1977, p 63-113
17. F. Eberle and J.H. Kitterman, *Behavior of Superheater Alloys in High Temperature, High Pressure Steam,* American Society of Mechanical Engineers, 1968, p 67
18. P.J. Grobner, C.C. Clark, P.V. Andreae, and W.R. Sylvester, Steamside Oxidation and Exfoliation of r-Mo Superheater and Reheater Steels, *NACE CORROSION 80,* Association of Corrosion Engineers, NACE, Houston, TX, 1980
19. K. Muramatsu, Development of Ultrasupercritical Plant in Japan, *Advanced Heat Resistant Steel for Power Generation,* R. Viswanathan and J.W. Nutting, Ed., IOM Communications, London, U.K., Book 708, p 543-559
20. K. Nakagawa, I. Kajigaya, T. Yanagisawa, M. Sato, and M. Abe, Study of Corrosion Resistance of Newly Developed 9-12%Cr Steels for Advanced Units, *Advanced Heat Resistance Steel for Power Generation,* R. Viswanathan and J.W. Nutting, Ed., Institute of Metals, London, U.K., 1999, p 468-481
21. H. Naoi, et al., NF616 Pipe Production and Properties and Welding Development in New Steels for Advanced Plant Up to 620 °C, E. Metcalfe, Ed., EPRI, Palo Alto, CA, 1995, p 8-30
22. W.J. Quadakkers, J. Ehlers, V. Shemet, and L. Singheiser, Development of Oxidation Resistant Ferritic Steels for Advanced High Efficiency Steam Power Plants, *Materials Aging and Life Management,* P. Rodriquez, Ed., Indiraganoy Centre for Atomic Research (IGCAR), Kalpakkam, India, October 3-6, 2000
23. A.S. Khanna, P. Rodriguez, J.B. Gnanamoorthy, Oxidation Kinetics, Breakaway Oxidation, and Inversion Phenomenon in 9Cr-1Mo Steels, *Oxid. Metals,* 1986, **26**(3-4), p 171-200
24. D.R. Holmes, D. Mortimer, and J. Newell, Corrosion of Steels in CO_2, *Proc. BNES,* Reading, 1974, p 151
25. J.W. Taylor and P.V. Trotsenberg, *Corrosion of Steels in CO_2*, *Proc. BNES,* Reading, 1974, p 180
26. Y. Fukuda and K. Tamura, Effect of Cr and Si Contents on the Steam Oxidation of High Cr Ferritic Steels, *Proc. Int. Symp. Plant Aging and Life Prediction of Corrodible Structures (*Sapporo, Japan), May 15-18, JSCE and NACE, 1995, p 835-840
27. K. Tamura, T. Sato, Y. Fukuda, K. Mitsuhata, and H. Yamanouchi, High Temperature Strength and Steam Oxidation Properties of New 9 approx 12% Cr Ferritic Steel Pipes for USC Boilers, *Proc. of the ASM 2nd Int. Conf. Heat Resistant Materials,* ASM, 1995, p 33-39
28. Y. Xu, Material Corrosion Under Supercritical and High Temperature Steam Conditions (Short Literature Survey), Kernforschungszentrum Karlsruhe, Germany, 1994
29. J.C. Griess, J.H. DeVan, W.A. Maxwell, Long-Term Corrosion of Cr-Ni Steels in Superheated Steam at 482 and 538 °C, *NACE CORROSION 81,* April (Toronto, Canada), NACE, Houston, TX, 1981
30. Y. Watanabe, Y.S. Yi, T. Kondo, K. Inui, T. Kishinami, H. Kimura, and M. Sato, *Proceedings of the 9th International Conference on Pressure Vessel Technology*, J. Price, Ed., ICPVT-9, April 9-14, 2000 (Sydney, Australia), p 545-552
31. H.L. Solberg, G.A. Hawkings, and A.A. Potter, Corrosion of Unstressed Steel Specimens and Various Metals by High-Temperature Steam, *Trans. ASME,* 1942, **64,** p 303-316
32. I.L. Kharina, V.M. Nikifrova, and A.V. Ryabchenkov, Effect of Si Content on the Oxidation Resistance of Low Alloyed Steel in Superheated Steam, *Z. Metall.,* 1968, **4**(5), p 570-574
33. T. Sato, Y. Fukuda, K. Mitsuhara, and K. Sakai, The Practical Application and Long-term Experience of New Heat Resistant Steels to Large Scale USC Boiler, *Advances in Materials Technology for Fossil Power Plants,* R. Viswanathan, D. Gandy, and K. Coleman, Ed., ASM International, 2005
34. M. Morinaga, Y. Murata, R. Hashizume, and Y. Sawaragi, Remarkable Improvement in Steam Oxidation Resistance due to the Presence of Sulfur in High Cr Ferritic Steels, *ISIJ Int.,* 2001, **41**(3), p 314-316
35. Y. Murata, M. Morinaga, R. Hashizume, Y. Sawaragi, and M. Nakoi, Role of Impurity Element on Steam Oxidation of High Cr Ferritic Steels in Advance in Materials Technology for Fossil Power Plants, R. Viswanathan, W.T. Bakker, and J.D. Parker, Ed., IOM Communications, London, U.K., 2001, p 267-375
36. M. Nakai, Y. Murata, M. Morinaga and R. Hashizuma, Dependence of High-Temperature Oxidation Resistance on the Stability of the Chromium Sulfide in High Chromium Heat Resistant Steels, *Hilton Head Conference Advances in Materials Technology for Fossil Power Plants,* R. Viswanathan, D. Gandy, and K. Coleman, Ed., ASM International, 2005, p 420-428
37. S. Osgerby and A. Fry, Assessment of the Steam Oxidation Behavior of High Temperature Plant Materials, *Hilton Head Conference Advances in Materials Technology for Fossil Power Plants,* R. Viswanathan, D. Gandy, and K. Coleman, Ed., ASM International, 2005
38. J. Ehlers, E.J. Smaardijk, H. Penkalla, A.K. Tyagi, L. Singheiser, and W.J. Quadakkers, Effect of Steel Composition on the Bell Shape Temperature Dependence of Oxidation in Water Vapor Containing Environments, *14th International Corrosion Congress (ICC) Proceedings,* October, 1999, p 336
39. F. Abe, M. Igarashi, S. Wanikawa, M. Tabuchi, T. Itagaki, K. Kimura, and K. Yamaguchi, New Ferritic Heat Resistance Steels for 650 °C USC Boilers, National Research Institute for Metals, Japan. Submitted to 3rd EPRI Conference in Swansea, U.K., April 2001
40. F. Abe, M. Igarashi, N. Fujitsuna, K. Kimura, and S. Muneki, Alloy Design of Advanced Ferritic Steels for 650 USC Boilers, *Advanced Heat Resistant Steel for Power Generation,* R. Viswanathan and J.W. Nutting, Ed., Institute of Materials, London, U.K., 1999, p 84-95
41. T. Itagaki, H. Kutsumi, M. Igarashi, and F. Abe, Alloy Design of Advanced Ferritic Steels in 650 °C USC Boiler, *ISJI,* 2000, **13,** p 1114-1115
42. F. Dettenwanger, M. Schorr, J. Ellrich, T. Weber, and M. Schutze, "The Influence of Si, W and Water Vapor on the Oxidation Behavior of 9Cr Steels," Paper 01151 presented at *NACE Corrosion 2001*, NACE, Houston, TX
43. P.N. Rowley, R. Brydson, J. Little, S.R.J. Saunders, H. Sauer, and W. Engel, The Effects of Boron Additions on the Oxidation of Fe-Cr Alloys in High Temperature Steam: Analytical Results and Mechanisms, *Oxid. Met.,* 1991, **35**(5/6), p 375-395
44. J.C. Griess, J.H. DeVan, and W.A. Maxwell, The Effect of High Heat Flux on the Oxidation of 2-1/4Cr-1Mo Steel Tubing in Superheated Steam, *Mater. Perf.,* 1980, **19**(6), p 46-52
45. A. Fry, S. Osgerby and M. Wright, "Oxidation of Alloys in Steam Environments – A Review," NPL Report, MATC(A)90 National Physical Laboratory, Teddington, U.K., July 2002
46. S. Osgerby and A. Fry, Simulating Steam Oxidation of High Temperature Plant under Laboratory Conditions: Practice and Interpretation of Data, NPL, U.K., June 2003, Personal Communication
47. P. Ennis and C. Filamonowicz, Recent Advances in Creep Resistant Steels for Power Plant Applications, *OMNI J.,* 2002, **1**(1), p 1-30
48. P. Ennis, Y. Wouters, and W.J. Quaddakers, The Effect of Oxidation on the Service Life of 9-12% Cr Steels, *Advanced Heat Resistant Steel for Power Generation,* R. Viswanathan and J.W. Nutting, Ed., IOM Communications, London, U.K., 1989, Book 708, pp 457-467
49. A. Fleming, R.V. Maskell, L.W. Buchanan, and T. Wilson, Material Developments for Supercritical Boilers and Pipework, *Materials for High-Temperature Power Generation and Process Plant Applications,* A. Strang, Ed, IOM Communications Limited, London, U.K., 2000, p 32-77
50. W.L. Pearl, E.G. Brush, G.G. Gaul, and S. Leistikow, General Corrosion of Inconel Alloy 625 in Simulated Superheat Reactor Environment, *Nuclear Appl.,* 1967, **3,** p 418-432
51. S. Mizuo and S. Toshiaki, et al., Corrosion Behavior of Austenitic Heat-Resistant Steels in High Temperature and High Pressure Steam Environment, *Tetsu-to-Hagane,* 1988, **74**(5), p 879-886
52. O. Yasuo, et al., Oxidation Behavior of Austenitic Heat-Resisting Steels in a High Temperature and High Pressure Steam Environment, *Trans. Iron Steel Inst. Japan,* 1988, **28**(9), p 761-768
53. K. Kanao, T. Kondo, K. Suzuki, Y. Watanabe, and Y. Yi, Steam Oxidation of Ferritic Heat-Resistant Steels for Ultra Supercritical Boilers, *Corros. Eng.,* 2001, **50**(2), p 50-56
54. H.E. McCoy and B. McNabb, Corrosion of Several Metals in Supercritical Steam at 538°C, ORNL-TM 5781 (1977)

55. S. Leistikow, Isothermal Steam Corrosion of Commercial Grade Austenitic Stainless Steels and Nickel Sase Alloys in Two Technical Surface Conditions, Proc. 4th International Congress Met. Cott. Amsterdam, NL (1969) pp 278-290
56. H.E. McCoy and B. McNabb, Corrosion of Several Iron- and Nickel-Base Alloys in Supercritical Steam at 1000 °F, *ORNL,* 1974, p TM-4552
57. S. Leistikow, A.V. Thenen, E. Pott, "Influence of Cold Work on Steam Corrosion of Five Ferritic Steels with Different Chromium Content," Technical Report KFK-2120
58. H. Matsuo, Y. Nishiyama, and T. Yamadera, Steam Oxidation of Fine-Grain Steels, *Advances in Materials Technology for Fossil Power Plants,* R. Viswanathan, D. Gandy, and K. Coleman, Ed., ASM International, 2005, p 441-451
59. H. Katsumi, H. Haruyama and F. Abe, Application of the Pre-Oxidation Treatment in Ar Gas for the NIMS High Strength Steels, Advances in Materials Technology for Fossil Power Plants, Ed. R. Viswanathan, D. Gandy and K. Coleman, ASM International, 2005
60. K. Yoshikawa, Scale Plugging Trouble of Superheater Tubes and Its Prevention, Central Research Laboratory Report, Sumitomo Metals Industries Limited, August 1974
61. N. Otsuka and H. Fujikawa, Scaling of Austenitic Stainless Steels and Nickel Base Alloys in High Temperature Steam at 973°K, *Corrosion,* 1991, **47**(4), p 240-248
62. W.L. Pearl and G.G. Gaul, General and Stress Corrosion of High Ni-alloys in Simulated Superheat Reactor Environment, GEAP-4165
63. Y. Nishiyama, Y. Hayaso, and N. Otsuka, Corrosion Resistant Boiler Tube Materials for Advanced Coal Fired Steam Generating Systems, *Proc. of the 28th International Conference on Coal Utilization,* March, 2003 (Clearwater, FL)
64. B.Y. Otoguro, et. al., Oxidation Behavior of Austenitic Heat Resisting Steels in High Temperature and High Pressure Steam Environment, *Trans ISIJ,* 28, 188, p 761-768
65. F. Masuyama, History Of Power Plants and Progress in Heat Resistant Steels, *ISIJ Int. J.,* 2001, **41**(6), p 612-625
66. P.H. Effertz and H. Meisel, Verzendureng Warmfeste Stahle Hochstrrukdampfel Nach IargenBetriebszeiten, (Damage to Machinery) *Der Machinenschaden,* 1971, **55**(1), p 14-20
67. P.L. Surman and J.E. Castle, Gas Phase Transport in the Oxidation of Iron and Steel, *Corros. Sci.,* 1969, **9,** p 771-778
68. N.J. Cory and T.M. Herrington, *Oxid. Metals*, 1987, **28** (5/6), p 237-258
69. P. Mayer and A.V. Manolescu, *High Temperature Corrosion*, R.A. Rapp, Ed., NACE, Houston, Texas, 1983, p 368-379
70. M.H. Davies, M.T. Simnad, and C.E. Birchenall, On the Mechanism and Kinetics of the Scaling of Iron, *J. Metals*, 1951, **3**(9), p 889-896
71. K. Heindelhofer and B.M. Larsen, Rates of Scale Formation on Iron and a Few of its Alloys, *Trans. Am. Soc. Steel Treating,* 1933, **21**(10), p 865-895
72. H.J. Yearian, E.C. Randall, and T.A. Longo, The Structure of Oxide Scales on Chromium Steels, *Corrosion,* 1956, **12**(10), p 515t-525t
73. P. Hurst and C. Cowan, Paper 62, presented at *Proc. International Conference on Ferritic Steels for Fast Breeder Steam Generators,* British Nuclear Energy Soc., 1977
74. Z. Zurek, S. Leistikow, and G. Schanz, Morphology and Chemical Composition of Scales Formed on Fe-11Cr Steel Oxidized in Steam at 900-1300°C, *Proceedings of the 8th European Congress on Corrosion,* November 19-21, 1985 (Paris, France)
75. R. Knodler and P.J. Ennis, Oxidation of High-Strength Ferritic Steels in Steam at 650°C: Preliminary Results of COST 522 Projects, *Proceedings of VTT Symposium, Baltica V,* Condition Assessment of Power Plant, P. Auerkari, Ed., June 6-8, 2001 (Finland), VTT, Helsinki, Finland, 2001, Vol. 1, p 355-364
76. K. Kusabiraki, H. Toki, and K. Asami, *Tetsu-to-Hagane,* 1988, **74,** p 863-878
77. K. Kinoshita, T. Mimino, and M. Shibata, Oxidation of Stainless Steel Tubing in High Temperature Steam, *Trans. Iron Steel Inst. Jpn.,* 1975, **15**(6), p 334-340
78. R. Blum and J. Hald, Benefit of Advanced Steam Power Plants, Materials for Advanced Power Engineering 2002, Lacomte-Becker, M. Carson, F. Schubert, and P.J. Ennis, Ed., Proceedings of the 7th Liege COST Conference, Part II, Forshoungszentrum Julich, Germany, p 1009-1017
79. I.M. Rehn, "Corrosion Problems in Coal Fired Boilers Superheater and Reheater Tubes: Steamside Oxidation and Exfoliation. Review and Results of Laboratory Tests." Final Report, *ASM,* **82-00,** 1981, p 143-162
80. B.A. Nevzorov, O.V. Starkov, and N.G. Baranov, "Characteristics of Elevated Temperature Oxidation of Steels in Steam, *Z. Metall.,* 1970, **6**(3), p 349-352
81. J. Armitt, R. Holmes, M.I. Manning, B. Meadowcraft, and E. Metcalfe, "The Spalling of Steam-Grown Oxide from Superheater and Reheater Tube Steels." EPRI Report TPS-76-655, February 1978 (Palo Alto, CA)
82. S. Osgerby and R.T. Fry, Simulating Steam Oxidation of High Temperature Plant under Laboratory Conditions: Practice and Interpretation of Data, *Mater. Res.,* 2004, **7,** p 141-146
83. S. Jansson, W. Hubner, G. Ostberg, and M. dePourbaix, Oxidation Resistance of Some Stainless Steels and Nickel-Based Alloys in High-Temperature Water and Steam, *Brit. Corros. J.*, 1969, **4**(1), p 21-31
84. M.G. Cox, B. McEnaney and V.D. Scott, Kinetics of Initial Oxide Growth on Fe-Cr Alloys and the Role of Vacancies in Film Breakdown, *Philos. Mag.,* 1975, **31**(2), p 331-338
85. N. Hussain, G. Schanz, S. Leistikow, and K.A. Shahid, High-Temperature Oxidation and Spalling Behavior of Incoloy 825, *Oxid. Met.,* 1989, **32**(5/6)**,** p 405-431
86. F. Masuyama, Alloy Development and Materials Issues, Advances in Materials Technology for Fossil Power Plants, R. Viswanathan, D.W. Gandy, and K. Coleman, Ed., ASM International, 2004, p 35-50
87. J.M. Sarver and J. Tanzosh, An Evaluation of the Steamside Oxidation of USC Materials at 650°C and 800°C, *Advances in Materials Technology for Fossil Power Plants,* R. Viswanathan, D. Gandy, and K. Coleman, Ed., ASM International, 2005
88. J.M. Sarver, as cited by S.I. Goodstine and J.C. Nava, USC on Surface Modification of Alloys for Ultra Supercritical Coal-fired Boilers, *Advances in Materials Technology for Fossil Power Plants,* R. Viswanathan, D. Gandy, and K. Coleman, ASM International, 2005